Available online at www.sciencedirect.com
SCIENCE DIRECT®
Journal of Sound and Vibration 289 (2006) 25–53
JOURNAL OF SOUND AND VIBRATION
www.elsevier.com/locate/jsvi

Vibration and dynamic response of functionally graded plates with piezoelectric actuators in thermal environments

Xiao-Lin Huang[1], Hui-Shen Shen*

School of Ocean and Civil Engineering, Shanghai Jiao Tong University, Shanghai 200030, People's Republic of China

Received 6 January 2004; received in revised form 29 December 2004; accepted 28 January 2005
Available online 4 May 2005

Abstract

This paper deals with the nonlinear vibration and dynamic response of a functionally graded material (FGM) plate with surface-bonded piezoelectric layers in thermal environments. Heat conduction and temperature-dependent material properties are both taken into account. The temperature field considered is assumed to be a uniform distribution over the plate surface and varied in the thickness direction of the plate, and the electric field is assumed to be the transverse component E_z only. Material properties of the substrate FGM layer are assumed to be temperature-dependent, and graded in the thickness direction according to a simple power-law distribution in terms of the volume fractions of the constituents, whereas the material properties of piezoelectric layers are assumed to be independent of the temperature and the electric field. The nonlinear formulations are based on the higher-order shear deformation plate theory and general von Kármán-type equation, which includes thermo-piezoelectric effects. The numerical illustrations concern nonlinear vibration characteristics of functional graded plates with fully covered piezoelectric actuators under different sets of thermal and electric loading conditions. The effects of temperature change, control voltage and volume fraction distribution on the nonlinear vibration and dynamic response are examined in detail.

*Corresponding author.
E-mail address: hsshen@mail.sjtu.edu.cn (H.-S. Shen).
[1]Now at Guilin University of Electronic Technology, Guilin 541004, People's Republic of China.

0022-460X/$ - see front matter © 2005 Elsevier Ltd. All rights reserved.
doi:10.1016/j.jsv.2005.01.033

Nomenclature

a, b length and width of a rectangular plate
d_{31}, d_{32} piezoelectric strain constants of a piezoelectric layer
A, **B**, **D**, **E**, **F**, **H** stiffness matrices
$A^*_{ij}, B^*_{ij}, D^*_{ij}, E^*_{ij}, F^*_{ij}, H^*_{ij}$ reduced stiffness matrices
E Young's modulus
$\bar{F}$ stress function
F dimensionless form of stress function
F^* dimensionless form of initial stress function
G shear modulus
h total thickness of a rectangular plate
h_f thickness of an FGM layer
h_p thickness of a piezoelectric layer
k, l, m, n displacement mode number
N volume fraction index
$\bar{N}_{IJ}, \bar{M}_{IJ}, \bar{P}_{IJ}$ forces, moments and higher-order moments
N_{IJ}, M_{IJ}, P_{IJ} dimensionless forms of forces, moments and higher-order moments
t time
T_U, T_L temperature on the upper and low surfaces of a rectangular plate
V_U, V_L applied voltage on the upper and low piezoelectric layers
$\bar{U}, \bar{V}, \bar{W}$ displacement components
U, V, W dimensionless forms of displacement components
W^* dimensionless form of initial deflection
α thermal expansion coefficient
κ_f thermal conductivity of an FGM layer
κ_p thermal conductivity of a piezoelectric layer
ν Poisson's ratio
$\bar{\omega}$ frequency
$\bar{\Psi}_x, \bar{\Psi}_y$ mid-plane rotations
Ψ_x, Ψ_y dimensionless forms of mid-plane rotations
Ψ^*_x, Ψ^*_y dimensionless forms of initial mid-plane rotations

1. Introduction

Functionally graded materials (FGMs) have gained considerably attention in engineering community, especially in high-temperature applications such as spacecraft and nuclear plants, due to their advantages of being able to withstand severe high-temperature gradient while maintain structural integrity. FGMs were initially designed as thermal barrier materials for aerospace structures and fusion reactors. They are now developed for the general use as structural components in high-temperature environments, and consequently many studies on thermo-mechanical characteristics of FGM plates are available in the literature, see, for example Refs. [1–6]. Liu and co-workers [7,8] studied numerically the mechanics problem for FGM plates in as earlier as 1991. Furthermore, they [9–11] analyzed the wave characteristics of functionally graded piezoelectric materials by using an inhomogeneous layer element method.

In recent years, with the increasing use of smart material such as piezoelectrics, shape alloys, and rheological fluids in vibration control of plate structures, the mechanical response of FGM plates with surface-bonded piezoelectric layers has attracted some researchers' attention. Among those, He et al. [12] and Liew et al. [13–15] presented the finite element formulation for the shape and vibration control of FGM plates with integrated actuators and sensors by using classical plate theory (CPT) and first-order shear deformable plate theory (FSDPT). Ootao and Tanigawa [16] studied the transient piezothermoelasticity of a functionally graded plate with surface-bonded piezoelectric layers on the basis of 3D elasticity. Reddy and Cheng [17] gave the 3D asymptotic

solutions for functionally graded plates with an active material layer to suppress the vibration amplitude by using the transfer matrix and asymptotic expansion technique. All the aforementioned studies focused on the linear vibration problems. In fact, when the plate deflection-to-thickness ratio is greater than 0.4, the nonlinearity is very important and should be put into consideration. Yang et al. [18] presented a large amplitude vibration analysis of an FGM plate with surface-bonded piezoelectric layers by using a semi-analytical method based on 1D differential quadrature and Galerkin technique. In their analysis, however, the heat conduction and/or temperature-dependent material properties are not accounted for.

The present work attempts to solve this problem, that is, to provide analytical solution for nonlinear free and forced vibration of FGM plates with surface-bonded piezoelectric layers in thermal environments. The temperature field is assumed to be constant in the plane and only varies in the thickness direction of the plate, and the electric field is assumed to be the transverse component E_z only. Material properties of the substrate FGM layer are assumed to be temperature-dependent, and graded in the thickness direction according to a simple power law distribution in terms of the volume fractions of the constituents, whereas the material properties of piezoelectric layers are assumed to be independent of the temperature and the electric field. The formulations, including thermo-piezoelectric effects, are based on Reddy's higher-order shear deformation plate theory [19] and general von Kármán-type equations [20–22]. An improved perturbation technique is employed to determine the nonlinear frequencies and dynamic responses of the hybrid FGM plate with surface-bonded piezoelectric layers. Due to the bending and stretching coupling effects, a nonlinear static problem is first solved to determine the pre-vibration deformation caused by temperature field and control voltage. By adding an incremental dynamic state to the pre-vibration state, the equations of motion are solved by an improved perturbation technique to determine nonlinear frequencies and dynamic responses of hybrid laminated plates. The parametric studies show the effects of volume fraction index, temperature change and control voltage on the natural frequency, nonlinear to linear frequency ratio and dynamic response of the hybrid FGM plate.

2. Theoretical development

The hybrid laminated plate considered herein comprises a substrate FGM layer with surface-bonded piezoelectric layers, as shown in Fig. 1. The substrate FGM layer is made from a mixture

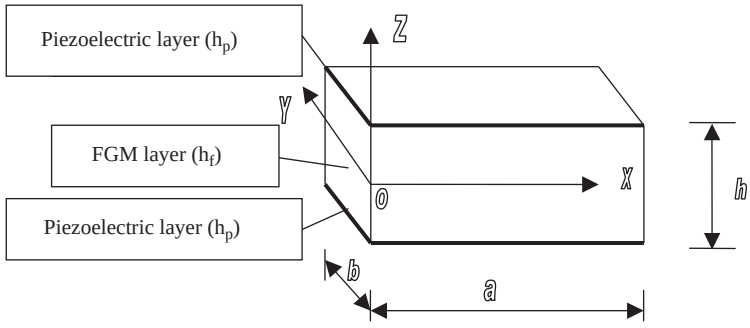

Fig. 1. Schematic diagram of a hybrid FGM plate.

of ceramics and metals. The length, width and total thickness of the hybrid laminated plate are a, b and h. The thickness of the FGM layer is h_f, while the thickness of each piezoelectric layer is h_p.

In order to accurately model the material properties of FGMs, the properties must be temperature-dependent and position-dependent. This is achieved by using a simple rule of mixture of composite materials. The effective material properties P_f of the FGM layer, like Young's modulus E_f, and thermal expansion coefficient α_f, can then be expressed as

$$P_f = \sum_{j=1} P_j V_{f_j}, \tag{1}$$

where P_j and V_{f_j} are the material properties and volume fraction of the constituent material j, and the sum of the volume fractions of all the constituent materials makes one, i.e.

$$\sum_{j=1} V_{f_j} = 1. \tag{2}$$

It is assumed that the constituent material properties can be expressed as a nonlinear function of temperature (see Ref. [23])

$$P_j = P_0(P_{-1}T^{-1} + 1 + P_1T + P_2T^2 + P_3T^3), \tag{3}$$

where P_0, P_{-1}, P_1, P_2 and P_3 are the coefficients of temperature T(K) and are unique to the constituent materials.

In addition, a simple power-law exponent of the volume fraction distribution is used to provide a measure of the amount of ceramic and metal in the FGM. In the present case, the volume fraction of ceramic is defined as

$$V_c(Z) = \left(\frac{2Z + h_f}{2h_f}\right)^N \tag{4}$$

in which volume fraction index N dictates the material variation profile through the FGM plate thickness and may be varied to obtain the optimum distribution of component materials.

We assume that the composition of the FGM layer is varied from the top to the bottom surface, i.e. the top surface ($Z = h_f/2$) of the plate is ceramic-rich whereas the bottom surface ($Z = -h_f/2$) is metal-rich. The effective Young's modulus E_f and thermal expansion coefficient α_f of the FGM layer are of temperature-dependent, whereas the mass density ρ_f, Poisson's ratio v_f and thermal conductivity κ_f are independent to the temperature. From Eqs. (1)–(4), one has

$$E_f(Z,T) = [E_t(T) - E_b(T)]\left(\frac{2Z + h_f}{2h_f}\right)^N + E_b(T), \tag{5a}$$

$$\alpha_f(Z,T) = [\alpha_t(T) - \alpha_b(T)]\left(\frac{2Z + h_f}{2h_f}\right)^N + \alpha_b(T), \tag{5b}$$

$$v_f(Z) = (v_t - v_b)\left(\frac{2Z + h_f}{2h_f}\right)^N + v_b, \tag{5c}$$

$$\rho_f(Z) = (\rho_t - \rho_b)\left(\frac{2Z + h_f}{2h_f}\right)^N + \rho_b, \tag{5d}$$

$$\kappa_f(Z) = (\kappa_t - \kappa_b)\left(\frac{2Z + h_f}{2h_f}\right)^N + \kappa_b \tag{5e}$$

in which subscripts 't' and 'b' imply the top and bottom surfaces of the FGM layer respectively.

We assume that the temperature variation occurs in the thickness direction only and 1D temperature field is assumed to be constant in the XY plane of the plate. In such a case, the temperature distribution along the thickness can be obtained by solving a steady-state heat transfer equation

$$-\frac{\mathrm{d}}{\mathrm{d}Z}\left[\kappa(Z)\frac{\mathrm{d}T}{\mathrm{d}Z}\right] = 0, \tag{6}$$

where

$$\kappa(Z) = \begin{cases} \kappa_p & (h_f/2 < Z < h_p + h_f/2), \\ \kappa_f(Z) & (-h_f/2 < Z < h_f/2), \\ \kappa_p & (-h_p - h_f/2 < Z < -h_f/2), \end{cases} \tag{7a}$$

$$T(Z) = \begin{cases} T_p(Z) & (h_f/2 \leqslant Z \leqslant h_p + h_f/2), \\ T_f(Z) & (-h_f/2 \leqslant Z \leqslant h_f/2), \\ \tilde{T}_p(Z) & (-h_p - h_f/2 \leqslant Z \leqslant -h_f/2), \end{cases} \tag{7b}$$

where κ_p is the thermal conductivity of piezoelectric layers. Eq. (6) is solved by imposing the boundary conditions

$$T_p\left(h_p + \frac{h_f}{2}\right) = T_U, \quad \tilde{T}_p\left(-h_p - \frac{h_f}{2}\right) = T_L \tag{8a}$$

and the continuity conditions

$$T_p(h_f/2) = T_f(h_f/2) = T_1, \quad T_f(-h_f/2) = \tilde{T}_p(-h_f/2) = T_2, \tag{8b}$$

$$\kappa_p \left.\frac{\mathrm{d}T_p(Z)}{\mathrm{d}Z}\right|_{Z=h_f/2} = \kappa_t \left.\frac{\mathrm{d}T_f(Z)}{\mathrm{d}Z}\right|_{Z=h_f/2}, \quad \kappa_p \left.\frac{\mathrm{d}\tilde{T}_p(Z)}{\mathrm{d}Z}\right|_{Z=-h_f/2} = \kappa_b \left.\frac{\mathrm{d}T_f(Z)}{\mathrm{d}Z}\right|_{Z=-h_f/2}. \tag{8c}$$

The solution of Eqs. (6)–(8) can be expressed as polynomial series [24]

$$T_p(Z) = T_1 + \frac{T_U - T_1}{h_p}(Z - h_f/2),$$

$$\tilde{T}_p(Z) = T_L + \frac{T_2 - T_L}{h_p}(Z + h_f/2 + h_p),$$

$$T_f(Z) = a_0 + a_1\left(\frac{2Z+h_f}{2h_f}\right) + a_2\left(\frac{2Z+h_f}{2h_f}\right)^{N+1} + a_3\left(\frac{2Z+h_f}{2h_f}\right)^{2N+1} + a_4\left(\frac{2Z+h_f}{2h_f}\right)^{3N+1} + a_5\left(\frac{2Z+h_f}{2h_f}\right)^{4N+1} + a_6\left(\frac{2Z+h_f}{2h_f}\right)^{5N+1} + O(Z)^{6N+1}, \tag{9}$$

where constants T_1, T_2 and a_j ($j = 0-6$) can be found in Appendix A.

From Eqs. (5a) and (5b), it can be seen that E_f and α_f are functions of temperature and position.

Suppose the plate is subjected to a transverse dynamic load $q(X, Y, t)$. The coordinate system has its origin at the corner of the plate on the middle plane. Let $\bar{U}$, $\bar{V}$ and $\bar{W}$ be the plate displacements parallel to a right-hand set of axes (X, Y, Z), where X is longitudinal and Z is perpendicular to the plate. $\bar{\Psi}_x$ and $\bar{\Psi}_y$ are the mid-plane rotations of the normals about the Y and X axes, respectively. Reddy [19] developed a simple higher-order shear deformation plate theory, in which the transverse shear strains are assumed to be parabolically distributed across the plate thickness and which contains the same dependent unknowns ($\bar{U}$, $\bar{V}$, $\bar{W}$, $\bar{\Psi}_x$ and $\bar{\Psi}_y$) as in the first-order shear deformation theory, but no shear correction factors are required. Based on Reddy's higher order shear deformation plate theory, Shen [20] derived a set of general von Kármán-type equations which can be expressed in terms of a transverse displacement $\bar{W}$, two rotations $\bar{\Psi}_x$ and $\bar{\Psi}_y$, and stress function $\bar{F}$ defined by $\bar{N}_x = \bar{F}_{,yy}$, $\bar{N}_y = \bar{F}_{,xx}$ and $\bar{N}_{xy} = -\bar{F}_{,xy}$, where a comma denotes partial differentiation with respect to the corresponding coordinates. These general von Kármán-type equations are successfully used in solving many nonlinear problems, e.g. nonlinear bending, postbuckling and nonlinear vibration of shear deformable laminated plates (see Refs. [25–27]). Following Shen [20], we can easily obtain the motion equations of the hybrid FGM plate including thermo-piezoelectric effects as

$$\begin{aligned}&\tilde{L}_{11}(\bar{W}) - \tilde{L}_{12}(\bar{\Psi}_x) - \tilde{L}_{13}(\bar{\Psi}_y) + \tilde{L}_{14}(\bar{F}) - \tilde{L}_{15}(\bar{N}^P) - \tilde{L}_{16}(\bar{M}^P)\\ &\quad = \tilde{L}(\bar{W}, \bar{F}) + \tilde{L}_{17}(\ddot{\bar{W}}) + I_8\left(\frac{\partial \ddot{\bar{\Psi}}_x}{\partial X} + \frac{\partial \ddot{\bar{\Psi}}_y}{\partial Y}\right) + q,\end{aligned} \tag{10}$$

$$\tilde{L}_{21}(\bar{F}) + \tilde{L}_{22}(\bar{\Psi}_x) + \tilde{L}_{23}(\bar{\Psi}_y) - \tilde{L}_{24}(\bar{W}) - \tilde{L}_{25}(\bar{N}^P) = -\frac{1}{2}\tilde{L}(\bar{W}, \bar{W}), \tag{11}$$

$$\tilde{L}_{31}(\bar{W}) + \tilde{L}_{32}(\bar{\Psi}_x) - \tilde{L}_{33}(\bar{\Psi}_y) + \tilde{L}_{34}(\bar{F}) - \tilde{L}_{35}(\bar{N}^P) - \tilde{L}_{36}(\bar{S}^P) = I_9\frac{\partial \ddot{\bar{W}}}{\partial X} + I_{10}\ddot{\bar{\Psi}}_x, \tag{12}$$

$$\tilde{L}_{41}(\bar{W}) - \tilde{L}_{42}(\bar{\Psi}_x) + \tilde{L}_{43}(\bar{\Psi}_y) + \tilde{L}_{44}(\bar{F}) - \tilde{L}_{45}(\bar{N}^P) - \tilde{L}_{46}(\bar{S}^P) = I_9\frac{\partial \ddot{\bar{W}}}{\partial Y} + I_{10}\ddot{\bar{\Psi}}_y \tag{13}$$

in which I_j and $\bar{I}_j$ are defined as in Huang and Zheng [27], and the linear operators $L_{ij}()$ and the nonlinear operator $L()$ are defined as in Refs. [21,22].

In the above equations, the superposed dots indicate differentiation with respect to time. The equivalent thermo-piezoelectric loads are defined as

$$\begin{bmatrix} \bar{N}^P \\ \bar{M}^P \\ \bar{S}^P \end{bmatrix} = \begin{bmatrix} \bar{N}^T \\ \bar{M}^T \\ \bar{S}^T \end{bmatrix} + \begin{bmatrix} \bar{N}^E \\ \bar{M}^E \\ \bar{S}^E \end{bmatrix}. \tag{14}$$

For the plate type piezoelectric material, only thickness direction electric field E_Z is dominant, and E_Z is defined as $E_Z = -\Phi_{,Z}$, where Φ is the potential field. If the voltage applied to the actuator in the thickness only, then

$$E_Z = \frac{V_k}{h_k}, \tag{15}$$

where V_k is the applied voltage across the kth ply and h_k ($k = 1$ and/or 3) is the thickness of the piezoelectric ply.

The forces, moments and higher-order moments caused by temperature or electric field are defined as

$$\begin{bmatrix} \bar{N}_x^T & \bar{M}_x^T & \bar{P}_x^T \\ \bar{N}_y^T & \bar{M}_y^T & \bar{P}_y^T \\ \bar{N}_{xy}^T & \bar{M}_{xy}^T & \bar{P}_{xy}^T \end{bmatrix} = \sum_k \int_{-h_{k-1}}^{h_k} \begin{bmatrix} A_x \\ A_y \\ A_{xy} \end{bmatrix}_k (1, Z, Z^3)\Delta T(Z)\,\mathrm{d}Z, \tag{16a}$$

$$\begin{bmatrix} \bar{S}_x^T \\ \bar{S}_y^T \\ \bar{S}_{xy}^T \end{bmatrix} = \begin{bmatrix} \bar{M}_x^T \\ \bar{M}_y^T \\ \bar{M}_{xy}^T \end{bmatrix} - \frac{4}{3h^2} \begin{bmatrix} \bar{P}_x^T \\ \bar{P}_y^T \\ \bar{P}_{xy}^T \end{bmatrix} \tag{16b}$$

or

$$\begin{bmatrix} \bar{N}_x^E & \bar{M}_x^E & \bar{P}_x^E \\ \bar{N}_y^E & \bar{M}_y^E & \bar{P}_y^E \\ \bar{N}_{xy}^E & \bar{M}_{xy}^E & \bar{P}_{xy}^E \end{bmatrix} = \sum_k \int_{-h_{k-1}}^{h_k} \begin{bmatrix} B_x \\ B_y \\ B_{xy} \end{bmatrix}_k (1, Z, Z^3)\frac{V_k}{h_k}\,\mathrm{d}Z, \tag{16c}$$

$$\begin{bmatrix} \bar{S}_x^E \\ \bar{S}_y^E \\ \bar{S}_{xy}^E \end{bmatrix} = \begin{bmatrix} \bar{M}_x^E \\ \bar{M}_y^E \\ \bar{M}_{xy}^E \end{bmatrix} - \frac{4}{3h^2} \begin{bmatrix} \bar{P}_x^E \\ \bar{P}_y^E \\ \bar{P}_{xy}^E \end{bmatrix}, \tag{16d}$$

where $\Delta T(Z) = T(Z) - T_0$ is temperature rise from the reference temperature T_0 at which there are no thermal strains, and

$$\begin{bmatrix} A_x \\ A_y \\ A_{xy} \end{bmatrix} = -\begin{bmatrix} Q_{11} & Q_{12} & Q_{16} \\ Q_{12} & Q_{22} & Q_{26} \\ Q_{16} & Q_{26} & Q_{66} \end{bmatrix} \begin{bmatrix} 1 & 0 \\ 0 & 1 \\ 0 & 0 \end{bmatrix} \begin{bmatrix} \alpha_{11} \\ \alpha_{22} \end{bmatrix}, \tag{17a}$$

$$\begin{bmatrix} B_x \\ B_y \\ B_{xy} \end{bmatrix} = -\begin{bmatrix} Q_{11} & Q_{12} & Q_{16} \\ Q_{12} & Q_{22} & Q_{26} \\ Q_{16} & Q_{26} & Q_{66} \end{bmatrix} \begin{bmatrix} 1 & 0 \\ 0 & 1 \\ 0 & 0 \end{bmatrix} \begin{bmatrix} d_{31} \\ d_{32} \end{bmatrix}, \tag{17b}$$

where α_{11}, α_{22} are the thermal expansion coefficients in the longitudinal and transverse directions, and d_{31} and d_{32} are piezoelectric strain constants of a piezoelectric ply, Q_{ij} are the transformed elastic constants, details of which can be found in Refs. [21,22]. Note that for FGM layer $\alpha_{11} = \alpha_{22} = \alpha_f(Z, T(Z))$ and

$$Q_{11} = Q_{22} = \frac{E_f(Z,T(Z))}{1-v_f^2(Z)}, \quad Q_{12} = \frac{v_f(Z)E_f(Z,T(Z))}{1-v_f^2(Z)},$$
$$Q_{16} = Q_{26} = 0, \quad Q_{44} = Q_{55} = Q_{66} = \frac{E_f(Z,T(Z))}{2(1+v_f(Z))}. \tag{18}$$

It is assumed that all four edges are simply supported with no in-plane displacements. The boundary conditions are

$X = 0, a$:

$$\bar{W} = \bar{\Psi}_y = 0, \tag{19a}$$

$$\bar{U} = 0. \tag{19b}$$

$Y = 0, b$:

$$\bar{W} = \bar{\Psi}_x = 0, \tag{19c}$$

$$\bar{V} = 0. \tag{19d}$$

Note that the stretching–bending coupling gives rise to bending curvatures under the action of in-plane loading, no matter how small these loads may be. In this situation the boundary condition of zero bending moment cannot be incorporated accurately, as reported in Ref. [21]. The conditions expressing the immovability conditions (19b) and (19d) are fulfilled on the average senses as (see Ref. [21])

$$\int_0^a \int_0^b \frac{\partial \bar{U}}{\partial X} \, \mathrm{d}X \, \mathrm{d}Y = 0, \tag{20a}$$

$$\int_0^b \int_0^a \frac{\partial \bar{V}}{\partial Y} \, \mathrm{d}Y \, \mathrm{d}X = 0 \tag{20b}$$

in which

$$\frac{\partial \bar{U}}{\partial X} = A_{11}^* \frac{\partial^2 \bar{F}}{\partial Y^2} + A_{12}^* \frac{\partial^2 \bar{F}}{\partial X^2} + \left(B_{11}^* - \frac{4}{3h^2} E_{11}^*\right) \frac{\partial \bar{\Psi}_x}{\partial X} + \left(B_{12}^* - \frac{4}{3h^2} E_{12}^*\right) \frac{\partial \bar{\Psi}_y}{\partial Y} - \frac{4}{3h^2}\left(E_{11}^* \frac{\partial^2 \bar{W}}{\partial X^2} + E_{12}^* \frac{\partial^2 \bar{W}}{\partial Y^2}\right) - \frac{1}{2}\left(\frac{\partial \bar{W}}{\partial X}\right)^2 - (A_{11}^* \bar{N}_x^P + A_{12}^* \bar{N}_y^P), \tag{21a}$$

$$\frac{\partial \bar{V}}{\partial Y} = A_{22}^* \frac{\partial^2 \bar{F}}{\partial X^2} + A_{12}^* \frac{\partial^2 \bar{F}}{\partial Y^2} + \left(B_{21}^* - \frac{4}{3h^2} E_{21}^*\right) \frac{\partial \bar{\Psi}_x}{\partial X} + \left(B_{22}^* - \frac{4}{3h^2} E_{22}^*\right) \frac{\partial \bar{\Psi}_y}{\partial Y} - \frac{4}{3h^2}\left(E_{21}^* \frac{\partial^2 \bar{W}}{\partial X^2} + E_{22}^* \frac{\partial^2 \bar{W}}{\partial Y^2}\right) - \frac{1}{2}\left(\frac{\partial \bar{W}}{\partial Y}\right)^2 - (A_{12}^* \bar{N}_x^P + A_{22}^* \bar{N}_y^P). \tag{21b}$$

In Eqs. (21a) and (21b), and what follows, $[A_{ij}^*]$, $[B_{ij}^*]$, $[D_{ij}^*]$, $[E_{ij}^*]$, $[F_{ij}^*]$ and $[H_{ij}^*]$ $(i,j = 1,2,6)$ are reduced stiffness matrices, determined through relationships

$$\mathbf{A}^* = \mathbf{A}^{-1}, \quad \mathbf{B}^* = -\mathbf{A}^{-1}\mathbf{B}, \quad \mathbf{D}^* = \mathbf{D} - \mathbf{B}\mathbf{A}^{-1}\mathbf{B}, \quad \mathbf{E}^* = -\mathbf{A}^{-1}\mathbf{E},$$
$$\mathbf{F}^* = \mathbf{F} - \mathbf{E}\mathbf{A}^{-1}\mathbf{B}, \quad \mathbf{H}^* = \mathbf{H} - \mathbf{E}\mathbf{A}^{-1}\mathbf{E}, \tag{22}$$

where A_{ij} , B_{ij} etc., are the plate stiffnesses, defined in the standard way [21].

3. Analytical method and asymptotic solutions

Having developed the theory, we will try to solve Eqs. (10)–(13) with boundary condition (19). Before proceeding, it is convenient to first define the following dimensionless quantities for the plate (with γ_{ijk} in Eq. (29) below defined as in Refs. [21,22]).

$$x = \pi X/a, \quad y = \pi Y/b, \quad z = Z/h, \quad \beta = a/b, \quad W = \bar{W}/[D_{11}^* D_{22}^* A_{11}^* A_{22}^*]^{1/4},$$

$$F = \bar{F}/[D_{11}^* D_{22}^*]^{1/2}, \quad (\Psi_x, \Psi_y) = (\bar{\Psi}_x, \bar{\Psi}_y)a/\pi[D_{11}^* D_{22}^* A_{11}^* A_{22}^*]^{1/4}, \quad \gamma_5 = -A_{12}^*/A_{22}^*,$$

$$\gamma_{14} = [D_{22}^*/D_{11}^*]^{1/2}, \quad \gamma_{24} = [A_{11}^*/A_{22}^*]^{1/2}, \quad (\gamma_{T1}, \gamma_{T2}) = (A_X^T, A_y^T)a^2/\pi^2[D_{11}^* D_{22}^*]^{1/2},$$

$$(\gamma_{P1}, \gamma_{P2}) = (B_x^E, B_y^E)a^2/\pi^2[D_{11}^* D_{22}^*]^{1/2},$$

$$(\gamma_{T3}, \gamma_{T4}, \gamma_{T6}, \gamma_{T7}) = (D_x^T, D_y^T, F_x^T, F_y^T)a^2/\pi^2 h^2 D_{11}^*$$

$$(\gamma_{P3}, \gamma_{P4}, \gamma_{P6}, \gamma_{P7}) = (D_x^E, D_y^E, F_x^E, F_y^E)a^2/\pi^2 h^2 D_{11}^*$$

$$(M_x, M_y, P_x, P_y, M_x^P, M_y^P, P_x^P, P_y^P) = (\bar{M}_x, \bar{M}_y, 4\bar{P}_x/3h^2, 4\bar{P}_y/3h^2, \bar{M}_x^P, \bar{M}_y^P, 4\bar{P}_x^P/3h^2, 4\bar{P}_y^P/3h^2)a^2/\pi^2 D_{11}^*[D_{11}^* D_{22}^* A_{11}^* A_{22}^*]^{1/4}$$

$$\tau = \frac{\pi t}{a}\sqrt{\frac{E_0}{\rho_0}}, \quad \gamma_{170} = -\frac{I_1 E_0 a^2}{\pi^2 \rho_0 D_{11}^*}, \quad \gamma_{171} = \frac{4E_0(I_5 I_1 - I_4 I_2)}{3\rho_0 h^2 I_1 D_{11}^*}$$

$$(\gamma_{80},\gamma_{90},\gamma_{10})=(I_8,I_9,I_{10})\frac{E_0}{\rho_0 D_{11}^*},\quad \lambda_q=qa^4/\pi^4 D_{11}^*[D_{11}^* D_{22}^* A_{11}^* A_{22}^*]^{1/4} \tag{23}$$

in which E_0 and ρ_0 are the reference values of E_b and ρ_b at the room temperature ($T_0=300\,\mathrm{K}$), respectively, and let

$$\begin{bmatrix} A_x^T & D_x^T & F_x^T \\ A_y^T & D_y^T & F_y^T \end{bmatrix}\bar{T}=-\sum_k \int_{h_{k-1}}^{h_k}\begin{bmatrix} A_x \\ A_y \end{bmatrix}_k (1,Z,Z^3)\Delta T(Z)\,\mathrm{d}Z, \tag{24a}$$

$$\begin{bmatrix} B_x^E & D_x^E & F_x^E \\ B_y^E & D_y^E & F_y^E \end{bmatrix}\Delta V=-\sum_k \int_{h_{k-1}}^{h_k}\begin{bmatrix} B_x \\ B_y \end{bmatrix}_k (1,Z,Z^3)\frac{V_k}{h_k}\,\mathrm{d}Z \tag{24b}$$

where $\bar{T}=(T_L+T_U-2T_0)/2$.

Eqs. (10)–(13) can then be re-written in the following dimensionless form:

$$\begin{aligned} &L_{11}(W)-L_{12}(\Psi_x)-L_{13}(\Psi_y)+\gamma_{14}L_{14}(F)-L_{16}(M^P)\\ &\quad=\gamma_{14}\beta^2 L(W,F)+L_{17}(\ddot{W})+\gamma_{80}\left(\frac{\partial\ddot{\Psi}_x}{\partial x}+\beta\frac{\partial\ddot{\Psi}_y}{\partial y}\right)+\lambda_q, \end{aligned} \tag{25}$$

$$L_{21}(F)+\gamma_{24}L_{22}(\Psi_x)+\gamma_{24}L_{23}(\Psi_y)-\gamma_{24}L_{24}(W)=-\frac{1}{2}\gamma_{24}\beta^2 L(W,W), \tag{26}$$

$$L_{31}(W)+L_{32}(\Psi_x)-L_{33}(\Psi_y)+\gamma_{14}L_{34}(F)-L_{36}(S^P)=\gamma_{90}\frac{\partial\ddot{W}}{\partial x}+\gamma_{10}\ddot{\Psi}_x, \tag{27}$$

$$L_{41}(W)-L_{42}(\Psi_x)+L_{43}(\Psi_y)+\gamma_{14}L_{44}(F)-L_{46}(S^P)=\gamma_{90}\beta\frac{\partial\ddot{W}}{\partial y}+\gamma_{10}\ddot{\Psi}_y, \tag{28}$$

where the dimensionless operators $L_{ij}()$ and $L()$ are defined as in Refs. [21,22].

The boundary conditions of Eq. (19) become

$x=0,\ \pi$:

$$W=\Psi_y=0, \tag{29a}$$

$$\begin{aligned} \int_0^\pi\int_0^\pi\Bigg[&\gamma_{24}^2\beta^2\frac{\partial^2 F}{\partial y^2}-\gamma_5\frac{\partial^2 F}{\partial x^2}+\gamma_{24}\left(\gamma_{511}\frac{\partial\Psi_x}{\partial x}+\gamma_{233}\beta\frac{\partial\Psi_y}{\partial y}\right)-\gamma_{24}\left(\gamma_{611}\frac{\partial^2 W}{\partial x^2}+\gamma_{244}\beta^2\frac{\partial^2 W}{\partial y^2}\right)\\ &-\frac{1}{2}\gamma_{24}\left(\frac{\partial W}{\partial x}\right)^2+(\gamma_{24}^2\gamma_{T1}-\gamma_5\gamma_{T2})\bar{T}+(\gamma_{24}^2\gamma_{P1}-\gamma_5\gamma_{P2})\Delta V\Bigg]\mathrm{d}x\,\mathrm{d}y=0. \end{aligned} \tag{29b}$$

$y=0,\ \pi$:

$$W=\Psi_x=0, \tag{29c}$$

$$\int_0^{\pi}\int_0^{\pi}\left[\frac{\partial^2 F}{\partial x^2}-\gamma_5\beta^2\frac{\partial^2 F}{\partial y^2}+\gamma_{24}\left(\gamma_{220}\frac{\partial \Psi_x}{\partial x}+\gamma_{522}\beta\frac{\partial \Psi_y}{\partial y}\right)-\gamma_{24}\left(\gamma_{240}\frac{\partial^2 W}{\partial x^2}+\gamma_{622}\beta^2\frac{\partial^2 W}{\partial y^2}\right)\right.$$
$$\left.-\frac{1}{2}\gamma_{24}\beta^2\left(\frac{\partial W}{\partial y}\right)^2+(\gamma_{T2}-\gamma_5\gamma_{T1})\bar{T}+(\gamma_{P2}-\gamma_5\gamma_{P1})\Delta V\right]\mathrm{d}y\,\mathrm{d}x=0. \tag{29d}$$

We assume that the solutions of Eqs. (25)–(29) can be expressed as

$$W(x,y,\tau)=W^*(x,y)+\tilde{W}(x,y,\tau),$$
$$\Psi_x(x,y,\tau)=\Psi_x^*(x,y)+\tilde{\Psi}_x(x,y,\tau),$$
$$\Psi_y(x,y,\tau)=\Psi_y^*(x,y)+\tilde{\Psi}_y(x,y,\tau),$$
$$F(x,y,\tau)=F^*(x,y)+\tilde{F}(x,y,\tau), \tag{30}$$

where $W^*(x,y)$ is an initial deflection due to initial thermo-piezoelectric bending moment, and $\tilde{W}(x,y,\tau)$ is an additional deflection. $\Psi_x^*(x,y)$, $\Psi_y^*(x,y)$ and $F^*(x,y)$ are the mid-plane rotations and stress function corresponding to $W^*(x,y)$. $\tilde{\Psi}_x(x,y,\tau)$, $\tilde{\Psi}_y(x,y,\tau)$ and $\tilde{F}(x,y,\tau)$ are defined analogously to $\Psi_x^*(x,y)$, $\Psi_y^*(x,y)$ and $F^*(x,y)$, but is for $\tilde{W}(x,y,\tau)$.

Due to the bending–stretching coupling effect in the FGM plate, the thermal preload will bring about deflections and bending curvatures which have significant influences on the plate vibration characteristics. To account for this effect, the pre-vibration solutions $W^*(x,y)$, $\Psi_x^*(x,y)$, $\Psi_y^*(x,y)$ and $F^*(x,y)$ are sought at the first step from the following nonlinear equations:

$$L_{11}(W^*)-L_{12}(\Psi_x^*)-L_{13}(\Psi_y^*)+\gamma_{14}L_{14}(F^*)-L_{16}(M^P)+\gamma_{14}\beta^2\left(p_x\frac{\partial^2 W^*}{\partial x^2}+p_y\frac{\partial^2 W^*}{\partial y^2}\right)$$
$$=\gamma_{14}\beta^2 L(W^*,F^*), \tag{31}$$

$$L_{21}(F^*)+\gamma_{24}L_{22}(\Psi_x^*)+\gamma_{24}L_{23}(\Psi_y^*)-\gamma_{24}L_{24}(W^*)=-\frac{1}{2}\gamma_{24}\beta^2 L(W^*,W^*), \tag{32}$$

$$L_{31}(W^*)+L_{32}(\Psi_x^*)-L_{33}(\Psi_y^*)+\gamma_{14}L_{34}(F^*)-L_{36}(S^P)=0, \tag{33}$$

$$L_{41}(W^*)-L_{42}(\Psi_x^*)+L_{43}(\Psi_y^*)+\gamma_{14}L_{44}(F^*)-L_{46}(S^P)=0. \tag{34}$$

In Eq. (31), p_x and p_y are edge compressive stresses induced by temperature change and control voltage with edge restraints. The solutions of Eqs. (31)–(34) can be assumed as

$$W^*(x,y)=\sum_{k=1,3,\ldots}\sum_{l=1,3,\ldots}w_{kl}\sin kx\sin ly,$$
$$\Psi_x^*(x,y)=\sum_{k=1,3,\ldots}\sum_{l=1,3,\ldots}(\psi_x)_{kl}\cos kx\sin ly,$$
$$\Psi_y^*(x,y)=\sum_{k=1,3,\ldots}\sum_{l=1,3,\ldots}(\psi_y)_{kl}\sin kx\cos ly,$$

$$F^*(x,y) = -\frac{1}{2}(B_{00}^{(0)}y^2 + b_{00}^{(0)}x^2) + \sum_{k=1,3,\ldots}\sum_{l=1,3,\ldots} f_{kl}\sin kx\sin ly. \tag{35}$$

We then expand the constant thermo-piezoelectric bending moments in the double Fourier sine series as

$$\begin{bmatrix} M_x^P & S_x^P \\ M_y^P & S_y^P \end{bmatrix} = -\begin{bmatrix} M_x^{(0)} & S_x^{(0)} \\ M_y^{(0)} & S_y^{(0)} \end{bmatrix} \sum_{k=1,3,\ldots}\sum_{l=1,3,\ldots} \frac{1}{kl}\sin kx\sin ly. \tag{36}$$

Substituting Eqs. (35) and (36) into Eqs. (31)–(34), applying Galerkin procedure to the Eqs. (31) and (32), W_{kl}, $(\psi_x)_{kl}$, $(\psi_y)_{kl}$ and f_{kl} can be determined, the detailed expressions are given in Appendix B.

Then $\tilde{W}(x,y,\tau)$, $\tilde{\Psi}_x(x,y,\tau)$, $\tilde{\Psi}_y(x,y,\tau)$ and $\tilde{F}(x,y,\tau)$ satisfy the nonlinear dynamic equations

$$L_{11}(\tilde{W}) - L_{12}(\tilde{\Psi}_x) - L_{13}(\tilde{\Psi}_y) + \gamma_{14}L_{14}(\tilde{F}) = \gamma_{14}\beta^2 L(\tilde{W}+W^*,\tilde{F}) + L_{17}(\ddot{\tilde{W}}) + \gamma_{80}\left(\frac{\partial\ddot{\tilde{\Psi}}_x}{\partial x} + \beta\frac{\partial\ddot{\tilde{\Psi}}_y}{\partial y}\right) + \lambda_q, \tag{37}$$

$$L_{21}(\tilde{F}) + \gamma_{24}L_{22}(\tilde{\Psi}_x) + \gamma_{24}L_{23}(\tilde{\Psi}_y) - \gamma_{24}L_{24}(\tilde{W}) = -\frac{1}{2}\gamma_{24}\beta^2 L(\tilde{W}+2W^*,\tilde{W}), \tag{38}$$

$$L_{31}(\tilde{W}) + L_{32}(\tilde{\Psi}_x) - L_{33}(\tilde{\Psi}_y) + \gamma_{14}L_{34}(\tilde{F}) = \gamma_{90}\frac{\partial\ddot{\tilde{W}}}{\partial x} + \gamma_{10}\ddot{\tilde{\Psi}}_x, \tag{39}$$

$$L_{41}(\tilde{W}) - L_{42}(\tilde{\Psi}_x) + L_{43}(\tilde{\Psi}_y) + \gamma_{14}L_{44}(\tilde{F}) = \gamma_{90}\beta\frac{\partial\ddot{\tilde{W}}}{\partial y} + \gamma_{10}\ddot{\tilde{\Psi}}_y. \tag{40}$$

The initial conditions are assumed to be

$$\tilde{W}|_{\tau=0} = \left.\frac{\partial\tilde{W}}{\partial\tau}\right|_{\tau=0} = 0, \tag{41a}$$

$$\tilde{\Psi}_x|_{\tau=0} = \left.\frac{\partial\tilde{\Psi}_x}{\partial\tau}\right|_{\tau=0} = 0, \tag{41b}$$

$$\tilde{\Psi}_y|_{\tau=0} = \left.\frac{\partial\tilde{\Psi}_y}{\partial\tau}\right|_{\tau=0} = 0. \tag{41c}$$

A perturbation technique is now used to solve Eqs. (37)–(41). The essence of this procedure, in the present case, is to assume that

$$\tilde{W}(x,y,\tilde{\tau},\varepsilon) = \sum_{j=1}\varepsilon^j W_j(x,y,\tilde{\tau}),$$

$$\tilde{F}(x,y,\tilde{\tau},\varepsilon) = \sum_{j=1}\varepsilon^j F_j(x,y,\tilde{\tau}),$$

$$\tilde{\Psi}_x(x,y,\tilde{\tau},\varepsilon)=\sum_{j=1}\varepsilon^j\Psi_{xj}(x,y,\tilde{\tau}),$$

$$\tilde{\Psi}_y(x,y,\tilde{\tau},\varepsilon)=\sum_{j=1}\varepsilon^j\Psi_{yj}(x,y,\tilde{\tau}),$$

$$\lambda_q(x,y,\tilde{\tau},\varepsilon)=\sum_{j=1}\varepsilon^j\lambda_j(x,y,\tilde{\tau}), \tag{42}$$

where ε is a small perturbation parameter. Here we introduce an important parameter $\tilde{\tau}=\varepsilon\tau$, which may be called a slow variable, to improve perturbation procedure for solving nonlinear dynamic problem.

Substituting Eq. (42) into Eqs. (37)–(40), and collecting terms of the same order of ε, a set of perturbation equations is obtained. Applying Galerkin procedure to the second equation of each order, and solving these equations step by step, we obtain asymptotic solutions, up to third order, as

$$\begin{aligned}\tilde{W}(x,y,\tau)=\varepsilon[w_1(\tau)+g_1\ddot{w}_1(\tau)]\sin mx\sin ny+(\varepsilon w_1(\tau))^3[\alpha g_{311}\sin mx\sin ny+g_{331}\sin 3mx\sin ny\\ +\ g_{313}\sin mx\sin 3ny]+O(\varepsilon^4),\end{aligned} \tag{43}$$

$$\begin{aligned}\tilde{\Psi}_x(x,y,\tau)=\varepsilon[g_{11}^{(1,1)}w_1(\tau)+g_2\ddot{w}_1(\tau)]\cos mx\sin ny+g_{12}(\varepsilon w_1(\tau))^2\sin 2mx\\ +\ (\varepsilon w_1(\tau))^3[\alpha g_{11}^{(1,1)}g_{311}\cos mx\sin ny+g_{11}^{(3,1)}g_{331}\cos 3mx\sin ny\\ +\ g_{11}^{(1,3)}g_{313}\cos mx\sin 3ny]+O(\varepsilon^4),\end{aligned} \tag{44}$$

$$\begin{aligned}\tilde{\Psi}_y(x,y,\tau)=\varepsilon[g_{21}^{(1,1)}w_1(\tau)+g_3\ddot{w}_1(\tau)]\sin mx\cos ny+g_{22}(\varepsilon w_1(\tau))^2\sin 2ny\\ +\ (\varepsilon w_1(\tau))^3[\alpha g_{21}^{(1,1)}g_{311}\sin mx\cos ny+g_{21}^{(3,1)}g_{331}\sin 3mx\cos ny\\ +\ g_{21}^{(1,3)}g_{313}\sin mx\cos 3ny]+O(\varepsilon^4),\end{aligned} \tag{45}$$

$$\begin{aligned}\tilde{F}(x,y,\tau)=\varepsilon[g_{31}^{(1,1)}w_1(\tau)+g_4\ddot{w}_1(\tau)]\sin mx\sin ny-\frac{1}{2}(\varepsilon w_1(\tau))^2(B_{00}^{(2)}y^2\\ +\ b_{00}^{(2)}x^2-2g_{402}\cos 2ny-2g_{420}\cos 2mx)+(\varepsilon w_1(\tau))^3[\alpha g_{31}^{(1,1)}g_{311}\sin mx\sin ny\\ +\ g_{31}^{(3,1)}g_{331}\sin 3mx\sin ny+g_{31}^{(1,3)}g_{313}\sin mx\sin 3ny]+O(\varepsilon^4),\end{aligned} \tag{46}$$

$$\begin{aligned}\lambda_q(x,y,\tau)=\varepsilon[g_{41}w_1(\tau)+g_{43}\ddot{w}_1(\tau)]\sin mx\sin ny+(\varepsilon w_1(\tau))^2(g_{441}\cos 2mx+g_{442}\cos 2ny)\\ -\ \gamma_{14}\beta^2(\varepsilon w_1(\tau))^2\sum_k\sum_l w_{kl}(B_{00}^{(2)}k^2+b_{00}^{(2)}l^2-4k^2n^2g_{402}\cos 2ny\\ -\ 4l^2m^2g_{420}\cos 2mx)\sin kx\sin ly+\bar{\alpha}g_{42}(\varepsilon w_1(\tau))^3\sin mx\sin ny+O(\varepsilon^4).\end{aligned} \tag{47}$$

Note that in Eqs. (43)–(47) $\tilde{\tau}$ is replaced by τ and for the case of free vibration $\alpha=0$, $\bar{\alpha}=1$, otherwise $\alpha=1$, $\bar{\alpha}=0$. Coefficients $g_{11}^{(i,j)}$, $g_{21}^{(i,j)}$, $g_{31}^{(i,j)}$ $(i,j=1,3)$, etc. are given in detail in Appendix B.

Then multiplying Eq. (47) by $(\sin mx \sin ny)$ and integrating over the plate area, one has

$$g_{43}\frac{d^2(\varepsilon w_1)}{d\tau^2}+g_{41}(\varepsilon w_1)+g_{44}(\varepsilon w_1)^2+\bar{\alpha}g_{42}(\varepsilon w_1)^3=\bar{\lambda}_q(\tau) \tag{48}$$

in which

$$\bar{\lambda}_q(\tau)=\frac{4}{\pi^2}\int_0^{\pi}\int_0^{\pi}\lambda_q(x,y,\tau)\sin mx\sin ny\,dx\,dy. \tag{49}$$

Substituting Eq. (30) into boundary condition (29), the coefficients $B_{00}^{(0)}$, $b_{00}^{(0)}$, $B_{00}^{(2)}$ and $b_{00}^{(2)}$ are then determined as given in Appendix B.

3.1. Free vibration

When $\bar{\alpha}=1$ and $\lambda_q(\tau)=0$, the Eq. (48) becomes the free vibration equation of the plate. The nonlinear frequency of the plate can be expressed as (see Ref. [28])

$$\omega_{\mathrm{NL}}=\omega_L\left[1+\frac{9g_{42}g_{41}-10g_{44}^2}{12g_{41}^2}A^2\right]^{1/2}. \tag{50}$$

In Eq. (50), $\omega_L=[g_{41}/g_{43}]^{1/2}$ is the dimensionless linear frequency, and $A=\bar{W}_{\max}/h$ is the amplitude to thickness ratio. According Eq. (23), the corresponding linear frequency can be expressed as $\bar{\omega}_L=\omega_L(\pi/a)(E_0/\rho_0)^{1/2}$, where E_0 and ρ_0 are defined as in Eq. (23).

3.2. Forced vibration

When the forced vibration is under consideration, we take $\bar{\alpha}=0$. In such a case, Eq. (48) can be re-written as

$$\varepsilon\ddot{w}_1(\tau)+\varepsilon w_1(\tau)\omega_L^2+\frac{g_{44}}{g_{43}}(\varepsilon w_1(\tau))^2+O(\varepsilon^4)=\frac{\bar{\lambda}_q(\tau)}{g_{43}}. \tag{51}$$

Eq. (51) may then be solved by using the Runge–Kutta iteration scheme (see Ref. [29])

$$\begin{aligned}(\varepsilon w_1)_{i+1}&=(\varepsilon w_1)_i+\Delta\tau(\varepsilon\dot{w}_1)_i+\frac{(\Delta\tau)^2}{6}(L_1+L_2+L_3),\\(\varepsilon\dot{w}_1)_{i+1}&=(\varepsilon\dot{w}_1)_i+\frac{\Delta\tau}{6}(L_1+2L_2+2L_3+L_4),\end{aligned} \tag{52}$$

where $\Delta\tau$ is the time step, and

$$\begin{aligned}L_1&=f(\tau_i,(\varepsilon w_1)),\quad L_2=f\left(\tau_i+\frac{\Delta\tau}{2},(\varepsilon w_1)_i+\frac{\Delta\tau(\varepsilon\dot{w}_1)_i}{2}\right),\\L_3&=f\left(\tau_i+\frac{\Delta\tau}{2},(\varepsilon w_1)_i+\frac{\Delta\tau(\varepsilon\dot{w}_1)_i}{2}+\frac{(\Delta\tau)^2}{4}L_1\right),\\L_4&=f\left(\tau_i+\Delta\tau,(\varepsilon w_1)_i+\Delta\tau(\varepsilon\dot{w}_1)_i+\frac{(\Delta\tau)^2}{2}L_2\right)\end{aligned} \tag{53}$$

in which

$$f(\tau, x) = -\omega_L^2 x - \frac{g_{44}}{g_{43}} x^2 + \frac{\bar{\lambda}_q(\tau)}{g_{43}}. \tag{54}$$

As a result, the solution of Eq. (51) is obtained numerically. Re-substituting it into Eqs. (43)–(47), both displacement and stress function are determined.

4. Numerical examples and discussion

A number of examples were solved to verify the present method. In all examples k and l in Eq. (35) are taken as 1, 3, and 5. In the present study, the adopted time step for Runge–Kutta direct iteration method was 2 μs.

4.1. Comparison studies

To ensure the accuracy and effectiveness of the present method, three test samples were solved for free and forced vibrations of FGM plates with or without piezoelectric layers.

Example 1. We first examine the static response of a simply supported FGM plate with symmetrically fully covered G-1195N piezoelectric layers. The substrate FGM layer consists of zirconia and aluminum. The top surface of the substrate FGM is ceramic-rich, whereas the bottom surface is metal-rich. The material properties adopted, as given in Ref. [14], are:

$$E_t = 151.0\,\text{GPa}, \quad v_t = 0.3, \quad \rho_t = 3000\,\text{kg/m}^3, \quad \kappa_t = 2.09\,\text{W/mk},$$
$$\alpha_t = 10 \times 10^{-6} \text{ for zirconia;}$$

$$E_b = 70.0\,\text{GPa}, \quad v_b = 0.3, \quad \rho_b = 2707\,\text{kg/m}^3, \quad \kappa_b = 204\,\text{W/mk},$$
$$\alpha_b = 23 \times 10^{-6} \text{ for aluminum;}$$

$$E_p = 63.0\,\text{GPa}, \quad v_p = 0.3, \quad \rho_p = 7600\,\text{kg/m}^3, \quad \kappa_p = 0.17\,\text{W/mk},$$
$$\alpha_p = 1.2 \times 10^{-4} \text{ for G-1195N.}$$

The side and thickness of the substrate FGM square plate are 400 and 10 mm, and the thickness of each piezoelectric lay is 0.1 mm. The temperature on the top surface is 20 °C, and on the bottom surface is 0 °C. The temperature is varied only in the thickness direction and determined by the steady-state heat conduction equation with boundary conditions. A stress free temperature $T_0 =$ 0 °C was taken. The curves of static centerline deflections for the hybrid FGM plate subjected to thermal loading were plotted in Fig. 2 and compared with the FEM results of Liew et al. [14] based on classic laminated plate theory (CLPT).

Example 2. We now consider the free vibration of an FGM square plate with symmetrically fully covered G-1195N piezoelectric layers. The substrate FGM plate is made of aluminum oxide and Ti–6Al–4V. The material properties adopted, as given in Ref. [12], are:

$$E_t = 320.24\,\text{GPa}, \quad v_t = 0.26, \quad \rho_t = 3750\,\text{kg/m}^3, \text{ for aluminum oxide;}$$

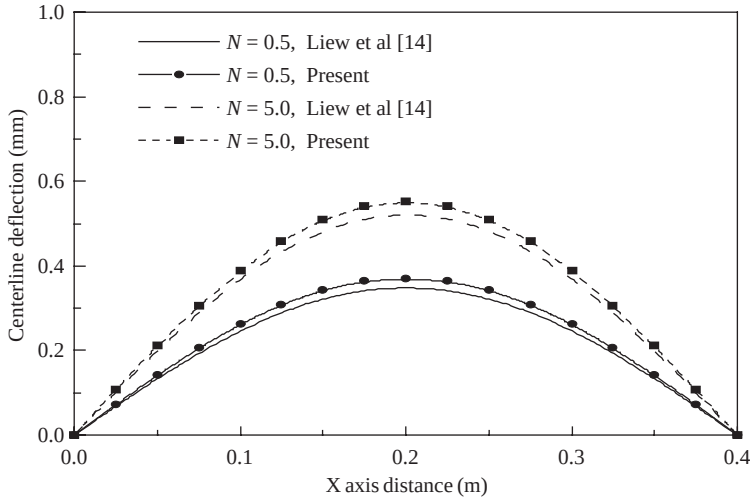

Fig. 2. Comparisons of centerline deflections for the hybrid FGM plate under thermal loading.

$$E_b = 105.70\,\text{GPa}, \quad \nu_b = 0.2981, \quad \rho_b = 4429\,\text{kg/m}^3, \text{ for Ti}-6\text{Al}-4\text{V};$$

$$E_p = 63.0\,\text{GPa}, \quad \nu_p = 0.3, \quad \rho_p = 7600\,\text{kg/m}^3, \quad d_{31} = d_{32} = 254 \times 10^{-12}\,\text{m/V}.$$

The side and thickness of the substrate FGM square plate are 400 and 5 mm, and the thickness of each piezoelectric lay is 0.1 mm. The initial ten frequencies of the plate as a function of the volume fraction index N are listed in Table 1 and compared with the FEM results of He et al. [12] based on classical laminated plate theory (CLPT).

Example 3. Finally, the curves of central deflection as functions of time for an FGM square plate subjected to a uniform sudden load $q_0 = -10^6\,\text{N/m}^2$ and in thermal environments are plotted and compared in Fig. 3 with the FEM results of Praveen and Reddy [1] based on first-order shear deformation plate theory (FDSPT). In Fig. 3, dimensionless central deflection and time are defined by $W = (\bar{W}E_m h/q_0 a^2)$ and $\tilde{t} = t[E_m/a^2\rho_m]^{1/2}$, respectively. In this example, the FGM plate is made of aluminum and alumina. The side and thickness of the square plate are 200 and 10 mm, respectively. The top surface is ceramic-rich, whereas the bottom surface is metal-rich. The temperature is varied only in the thickness direction and determined by the steady-state heat conduction equation with the boundary conditions. A stress free temperature $T_0 = 0\,^\circ\text{C}$ was taken. The material properties adopted, as given in Ref. [1], are

$$E_b = 70\,\text{GPa}, \quad \nu_b = 0.3, \quad \rho_b = 2707\,\text{kg/m}^3, \quad \alpha_b = 23.0 \times 10^{-6}/^\circ\text{C},$$
$$\kappa_b = 204\,\text{W/mK}, \text{ for aluminum},$$

$$E_t = 380\,\text{GPa}, \quad \nu_t = 0.3, \quad \rho_t = 3800\,\text{kg/m}^3, \quad \alpha_t = 7.4 \times 10^{-6}/^\circ\text{C},$$

$$\kappa_t = 10.4\,\text{W/mK}, \text{ for alumina}.$$

Table 1
Comparisons of natural frequency $\bar{\omega}_L$ (Hz) for simply supported FGM plates with actuator layers bonded on the top and bottom surfaces

Mode	Method	$N=0$	$N=0.5$	$N=1$	$N=5$	$N=15$	$N=100$	$N=1000$
1	He et al. [12]	144.25	185.45	198.92	230.46	247.30	259.35	261.73
	Present	143.25	184.73	198.78	229.47	246.86	258.78	260.84
2	He et al. [12]	359.00	462.65	495.62	573.82	615.58	645.55	651.49
	Present	358.87	461.02	494.65	571.87	613.95	643.92	649.83
3	He et al. [12]	359.00	462.47	495.62	573.82	615.58	645.55	651.49
	Present	358.87	461.02	494.65	571.87	613.95	643.92	649.83
4	He et al. [12]	564.10	731.12	778.94	902.04	967.78	1014.94	1024.28
	Present	563.42	727.98	778.61	899.91	964.31	1012.54	1023.72
5	He et al. [12]	717.80	925.45	993.11	1148.12	1231.00	1290.78	1302.64
	Present	717.65	922.83	992.87	1146.87	1229.44	1288.73	1301.34
6	He et al. [12]	717.80	925.45	993.11	1148.12	1231.00	1290.78	1302.64
	Present	717.65	922.83	992.87	1146.87	1229.44	1288.73	1301.34
7	He et al. [12]	908.25	1180.93	1255.98	1453.32	1558.77	1634.65	1649.70
	Present	907.87	1177.34	1223.36	1451.66	1557.12	1632.18	1648.56
8	He et al. [12]	908.25	1180.93	1255.98	1453.32	1558.77	1634.65	1649.70
	Present	907.87	1177.34	1223.36	1451.66	1557.12	1632.18	1648.56
9	He et al. [12]	1223.14	1576.91	1697.15	1958.17	2097.91	2199.46	2219.67
	Present	1219.32	1571.65	1695.17	1956.79	2095.67	2197.47	2217.94
10	He et al. [12]	1223.14	1576.91	1697.15	1958.17	2097.91	2199.46	2219.67
	Present	1219.32	1571.65	1695.17	1956.79	2095.67	2197.47	2217.94

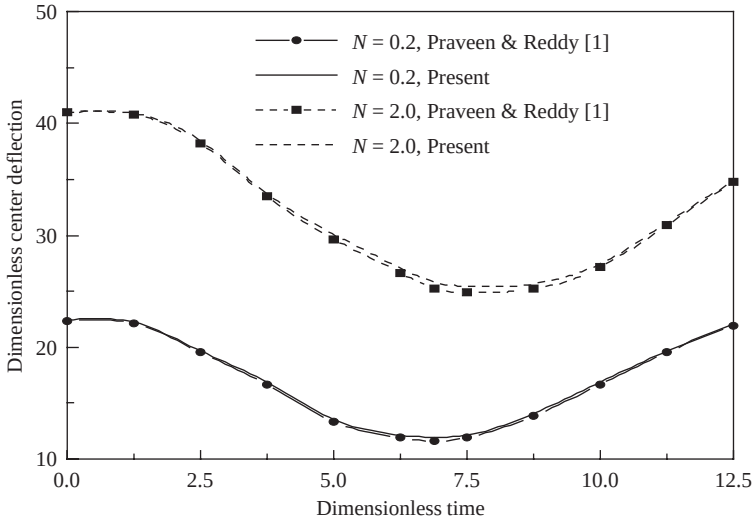

Fig. 3. Comparisons of central deflection versus time curves for an FGM square plate subjected to a sudden load in thermal environments.

Good agreement can be seen in these three comparisons. Note that in these examples the material properties are assumed to be independent of temperature.

4.2. Parametric studies

Parametric studies have been performed to study the nonlinear vibration and dynamic response of hybrid FGM plates subjected to the combined action of transverse dynamic load, electric load and thermal loading. Two types of the hybrid FGM plate are considered. The first hybrid FGM plate has fully covered piezoelectric actuators on the top surface (referred to as P/FGM), and the second has two piezoelectric layers symmetrically bonded to the top and bottom surfaces (referred to as P/FGM/P). Silicon nitride (Si_3N_4) and stainless steel (SUS304) are chosen to be the constituent materials of the substrate FGM layer, and the upper surface of the FGM plate is ceramic-rich and the lower surface is metal-rich. The thickness of the substrate FGM layer $h_f = 1.0\,\text{mm}$ and the thickness of each piezoelectric layer $h_p = 0.1\,\text{mm}$. The side of the hybrid FGM plate is $a = b = 24\,\text{mm}$. The mass density, Poisson's ratio and thermal conductivity are $2370\,\text{kg/m}^3$, $0.24, 9.19\,\text{W/mK}$ for Si_3N_4, and $8166\,\text{kg/m}^3$, $0.33, 12.04\,\text{W/mK}$ for SUS304. Young's modulus and the coefficient of thermal expansion are assumed to be dependent on the temperature and listed in Table 2. The material properties of the piezoelectric layers (PZT-5A) are $E_p = 63.0\,\text{GPa}$, $G_p = 24.2\,\text{GPa}$, $\nu_p = 0.3$, $\alpha_{11} = \alpha_{22} = 0.9 \times 10^{-6}/\text{K}$, $\kappa_p = 2.1\,\text{W/mk}$, $\rho_p = 7600\,\text{kg/m}^3$ and $d_{31} = d_{32} = 2.54 \times 10^{-10}\,\text{m/V}$.

The temperature field is assumed to vary only in the thickness direction of the plate and may be determined by the steady-state heat conduction equation with thermal boundary conditions and continuity conditions across the plate thickness. A stress-free temperature $T_0 = 300\,\text{K}$ was used.

Typical results are listed in Tables 3–6 and plotted in Figs. 4–7, for which the dynamic load is assumed to be a suddenly applied uniform load with $q_0 = 2\,\text{MPa}$. Six different applied voltages: $V_U = -200\,\text{V}$, $V_U = 0\,\text{V}$, $V_U = 200\,\text{V}$, and $V_L = V_U = -200\,\text{V}$, $V_L = V_U = 0\,\text{V}$, $V_L = V_U = 200\,\text{V}$ are used, where subscripts 'L' and 'U' imply the low and upper piezoelectric layer.

Table 3 shows the effect of volume fraction index N, control voltage and temperature field on the natural frequency parameter $\Omega = \bar{\omega}_L h\sqrt{E_0/\rho_0}/a^2$ of the two types of the hybrid FGM plate. E_0 and ρ_0 are defined as in Eq. (23). It can be seen that the natural frequency of these two plates is decreased by increasing temperature and volume fraction index N. The plus voltage decreases, but the minus voltage increases the plate natural frequency.

Tables 4–6 show, respectively, the effect of volume fraction index N, control voltage and temperature field on the nonlinear to linear frequency ratios $\omega_{\text{NL}}/\omega_L$ of these two hybrid FGM

Table 2
Temperature-dependent coefficients for ceramic and metals, from Reddy and Chin [30]

Materials	Properties	P_0	P_{-1}	P_1	P_2	P_3
Si_3N_4	E (Pa)	348.43e + 9	0.0	−3.070e−4	2.160e−7	−8.964e−11
	α (1/K)	5.8723e−6	0.0	9.095e−4	0.0	0.0
SUS304	E (Pa)	201.04e + 9	0.0	3.079e−4	−6.534e−7	0.0
	α (1/K)	12.330e−6	0.0	8.086e−4	0.0	0.0

Table 3
Natural frequency parameter $\Omega = \bar{\omega}_L(a^2/h_f)[\rho_0/E_0]^{1/2}$ for the hybrid FGM plates under different sets of thermal and electric loading conditions

Stacking sequence	Temperature environment	Applied voltage	Volume fraction index				
			Si_3N4	0.5	2.0	4.0	SUS304
(P/FGM)	$T_L = 300\,K$						
	$T_U = 300\,K$	$V_U = -200\,V$	12.485	9.120	7.223	6.718	5.897
		$V_U = 0\,V$	12.460	9.100	7.206	6.710	5.879
		$V_U = 200\,V$	12.435	9.080	7.189	6.702	5.861
	$T_U = 400\,K$	$V_U = -200\,V$	11.705	8.455	6.623	6.127	5.252
		$V_U = 0\,V$	11.682	8.438	6.608	6.113	5.237
		$V_U = 200\,V$	11.658	8.421	6.595	6.101	5.224
	$T_U = 600\,K$	$V_U = -200\,V$	10.128	7.222	5.632	5.215	4.717
		$V_U = 0\,V$	10.123	7.215	5.612	5.191	4.674
		$V_U = 200\,V$	10.120	7.213	5.595	5.169	4.624
(P/FGM/P)	$T_L = 300\,K$						
	$T_U = 300\,K$	$V_U = V_L = -200\,V$	11.675	8.869	7.217	6.768	5.779
		$V_U = V_L = 0\,V$	11.661	8.830	7.181	6.733	5.744
		$V_U = V_L = 200\,V$	11.649	8.790	7.144	6.697	5.711
	$T_U = 400\,K$	$V_U = V_L = -200\,V$	10.721	7.905	6.304	5.848	4.867
		$V_U = V_L = 0\,V$	10.716	7.860	6.262	5.807	4.829
		$V_U = V_L = 200\,V$	10.720	7.815	6.221	5.766	4.788
	$T_U = 600\,K$	$V_U = V_L = -200\,V$	8.544	5.713	4.434	4.221	1.594
		$V_U = V_L = 0\,V$	8.529	5.671	4.417	4.212	1.442
		$V_U = V_L = 200\,V$	8.514	5.629	4.399	4.211	1.289

Table 4
Effect of volume fraction index N on nonlinear to linear frequency ratio ω_{NL}/ω_L for the hybrid FGM plates in thermal environments ($T_L = 300\,K$, $T_U = 400\,K$)

	$\bar{W}_{max}/h$					
	0.0	0.2	0.4	0.6	0.8	1.0
(P/FGM) ($V_U = 200\,V$)						
Si_3N_4	1.000	1.022	1.084	1.180	1.302	1.445
0.5	1.000	1.022	1.086	1.184	1.311	1.457
2.0	1.000	1.023	1.088	1.186	1.313	1.459
4.0	1.000	1.023	1.089	1.188	1.316	1.462
SUS304	1.000	1.024	1.091	1.190	1.319	1.467
(P/FGM/P) ($V_L = V_U = 200\,V$)						
Si_3N_4	1.000	1.022	1.086	1.181	1.304	1.447
0.5	1.000	1.023	1.088	1.189	1.316	1.465
2.0	1.000	1.024	1.090	1.191	1.319	1.468
4.0	1.000	1.024	1.091	1.193	1.326	1.479
SUS304	1.000	1.025	1.096	1.208	1.344	1.504

Table 5
Effect of temperature field on nonlinear to linear frequency ratio ω_{NL}/ω_L for the hybrid FGM plates ($N = 0.5$)

	$\bar{W}_{max}/h$					
	0.0	0.2	0.4	0.6	0.8	1.0
(P/FGM) ($V_U = 200$ V)						
$T_L = 300$ K $T_U = 300$ K	1.000	1.019	1.075	1.163	1.275	1.406
$T_L = 300$ K $T_U = 400$ K	1.000	1.022	1.086	1.184	1.311	1.456
$T_L = 300$ K $T_U = 600$ K	1.000	1.025	1.097	1.206	1.345	1.505
(P/FGM) ($V_U = V_L = 200$ V)						
$T_L = 300$ K $T_U = 300$ K	1.000	1.018	1.071	1.185	1.261	1.387
$T_L = 300$ K $T_U = 400$ K	1.000	1.023	1.088	1.190	1.319	1.469
$T_L = 300$ K $T_U = 600$ K	1.000	1.033	1.128	1.270	1.446	1.644

Table 6
Effect of applied voltage on nonlinear to linear frequency ratio ω_{NL}/ω_L for the hybrid FGM plates in thermal environments ($T_L = 300$ K $T_U = 400$ K, $N = 2.0$)

	$\bar{W}_{max}/h$					
	0.0	0.2	0.4	0.6	0.8	1.0
(P/FGM)						
$V_U = -200$ V	1.000	1.021	1.083	1.178	1.300	1.441
$V_U = 0$ V	1.000	1.021	1.083	1.179	1.301	1.442
$V_U = 200$ V	1.000	1.021	1.083	1.179	1.301	1.443
(P/FGM)						
$V_U = V_L = -200$ V	1.000	1.022	1.084	1.182	1.305	1.449
$V_U = V_L = 0$ V	1.000	1.022	1.086	1.184	1.309	1.454
$V_U = V_L = 200$ V	1.000	1.022	1.087	1.186	1.313	1.459

plates. It can be seen that the ratios ω_{NL}/ω_L increase as the volume fraction index N or temperature increases. It is noted that the control voltage only has a small effect on the frequency ratios.

Figs. 4 and 5 show, respectively, the effect of volume fraction index N and temperature change on the dynamic response of the P/FGM plate. The results show that the dynamic deflections of the P/FGM plate are increased by increasing volume fraction index N and temperature change, this is because the stiffness of the plate becomes weaker when the temperature or volume fraction index N is increased. They also show that the greater the temperature change and volume fraction index N are, the greater the initial bending moments will be.

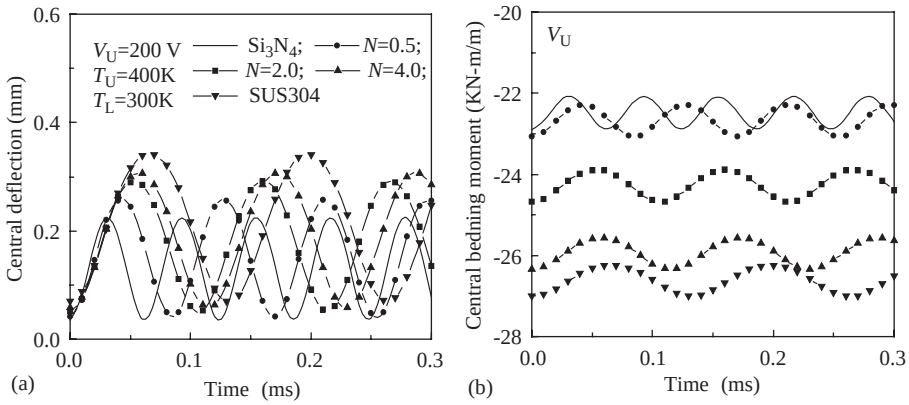

Fig. 4. Effect of volume fraction index N on the dynamic response of P/FGM plate subjected to a sudden load, control voltage and in thermal environments. (a) Central deflection versus time; (b) central bending moment versus time.

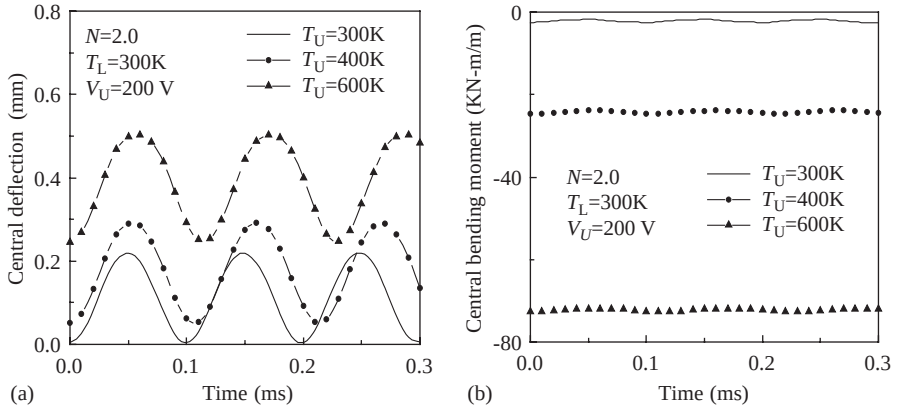

Fig. 5. Effect of thermal environmental conditions on the dynamic response of P/FGM square plate subjected to a sudden load and control voltage. (a) Central deflection versus time; (b) central bending moment versus time.

Fig. 6 shows the effect of control voltage on the dynamic response of the same plate. The results show that the control voltage has a significant effect on the initial bending moment, but it affects the dynamic deflection insignificantly.

Fig. 7 compares the dynamic response of the P/FGM and P/FGM/P plates. It can be seen that the central deflection and the bending moment of the P/FGM plate are higher than those of the P/FGM/P plate under the same loading condition.

5. Concluding remarks

Nonlinear free and forced vibration analyses have been presented for simply supported, hybrid FGM plates subjected to the combined action of transverse dynamic load, electric load and

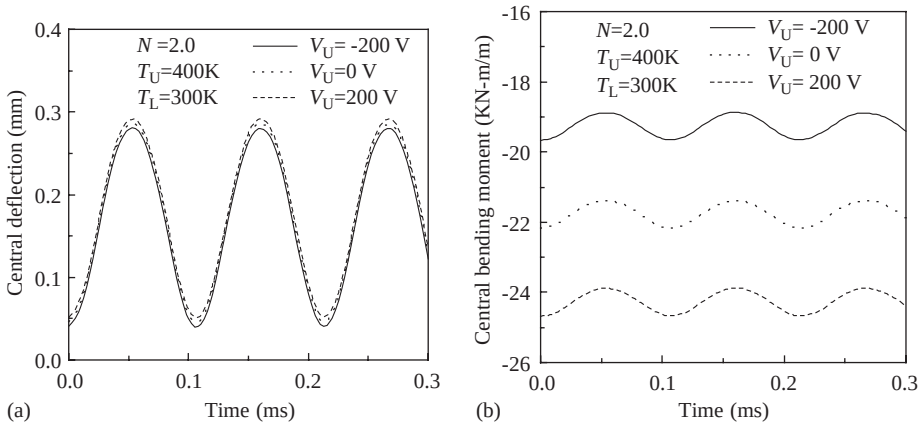

Fig. 6. Effect of control voltage on the dynamic response of P/FGM square plate subjected to a sudden load in thermal environments. (a) Central deflection versus time; (b) central bending moment versus time.

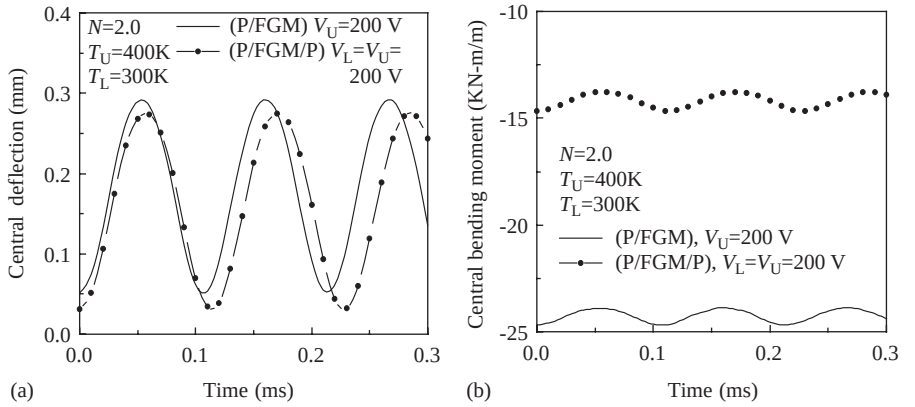

Fig. 7. Comparisons of the dynamic response of the P/FGM and P/FGM/P plates subjected a uniform sudden load, control voltage and in thermal environments. (a) Central deflection versus time; (b) central bending moment versus time.

thermal loading. Heat conduction and temperature-dependent material properties are both taken into account. The formulations are based on higher-order shear deformation plate theory and general von Kármán-type equations, and include thermo-piezoelectric effects. Analytical solutions have been presented by using an improved perturbation technique. A parametric study for hybrid FGM plates with different values of volume fraction index and under different sets of electric and thermal loading conditions has been carried out. Numerical results show that the natural frequencies are reduced by increasing the volume fraction index N, temperature change and plus control voltage, but increased by minus control voltage. The results also confirm that the temperature field and the volume fraction distribution have a significant effect on the dynamic response of hybrid FGM plates. In contrast, the control voltage only has a small effect on the dynamic response.

Acknowledgements

This work is supported in part by the National Natural Science Foundation of China under Grant 50375091. The authors are grateful for this financial support.

Appendix A

In Eqs. (9)

$$T_1 = T_2 + (T_U - T_L) - \frac{\kappa_t d + \kappa_b}{\kappa_b}(T_2 - T_L), \quad T_2 = T_L + \frac{\dfrac{\kappa_b}{ch_f}(T_U - T_L)}{\dfrac{\kappa_p}{h_p} + \dfrac{\kappa_t d + \kappa_b}{ch_f}},$$

$$a_0 = T_2, \quad a_1 = \frac{T_1 - T_2}{c}, \quad a_2 = -\frac{T_1 - T_2}{c}\frac{\kappa_{tb}}{(N+1)\kappa_b}, \quad a_3 = \frac{T_1 - T_2}{c}\frac{\kappa_{tb}^2}{(2N+1)\kappa_b^2},$$

$$a_4 = -\frac{T_1 - T_2}{c}\frac{\kappa_{tb}^3}{(3N+1)\kappa_b^3}, \quad a_5 = \frac{T_1 - T_2}{c}\frac{\kappa_{tb}^4}{(4N+1)\kappa_b^4}, \quad a_6 = -\frac{T_1 - T_2}{c}\frac{\kappa_{tb}^6}{(6N+1)\kappa_b^6}, \tag{A.1}$$

where

$$\begin{aligned}
\kappa_{tb} &= \kappa_t - \kappa_b,\\
c &= 1 - \frac{1}{N+1}\frac{\kappa_{tb}}{\kappa_b} + \frac{1}{2N+1}\left(\frac{\kappa_{tb}}{\kappa_b}\right)^2 - \frac{1}{3N+1}\left(\frac{\kappa_{tb}}{\kappa_b}\right)^3\\
&\quad + \frac{1}{4N+1}\left(\frac{\kappa_{tb}}{\kappa_b}\right)^4 - \frac{1}{5N+1}\left(\frac{\kappa_{tb}}{\kappa_b}\right)^5,\\
d &= 1 - \frac{\kappa_{tb}}{\kappa_b} + \left(\frac{\kappa_{tb}}{\kappa_b}\right)^2 - \left(\frac{\kappa_{tb}}{\kappa_b}\right)^3 + \left(\frac{\kappa_{tb}}{\kappa_b}\right)^4 - \left(\frac{\kappa_{tb}}{\kappa_b}\right)^5.
\end{aligned} \tag{A.2}$$

Appendix B

In Eq. (35)

$$\begin{aligned}
w_{kl} &= \sqrt[3]{-\frac{q_{kl}}{2} + \sqrt{\frac{(q_{kl})^2}{4} + \frac{(p_{kl})^3}{27}}} + \sqrt[3]{-\frac{q_{kl}}{2} - \sqrt{\frac{(q_{kl})^2}{4} + \frac{(p_{kl})^3}{27}}},\\
f_{kl} &= c_{31}^{(k,l)} w_{kl}^2 + c_{32}^{(k,l)} w_{kl} + c_{33}^{(k,l)},\\
(\psi_x)_{kl} &= c_{11}^{(k,l)} w_{kl} + c_{12}^{(k,l)} f_{kl} + c_{13}^{(k,l)}, \quad (\psi_y)_{kl} = c_{21}^{(k,l)} w_{kl} + c_{22}^{(k,l)} f_{kl} + c_{23}^{(k,l)},
\end{aligned} \tag{B.1}$$

where

$$(c_{11}^{(k,l)}, c_{12}^{(k,l)}, c_{13}^{(k,l)}) = \frac{1}{b_{32}^{(k,l)} b_{43}^{(k,l)} - b_{42}^{(k,l)} b_{33}^{(k,l)}}(b_{41}^{(k,l)} b_{33}^{(k,l)} - b_{31}^{(k,l)} b_{43}^{(k,l)}, b_{44}^{(k,l)} b_{33}^{(k,l)} - b_{34}^{(k,l)} b_{43}^{(k,l)}, y_3 b_{43}^{(k,l)} - y_4 b_{33}^{(k,l)}),$$

$$(c_{21}^{(k,l)}, c_{22}^{(k,l)}, c_{23}^{(k,l)}) = \frac{1}{b_{33}^{(k,l)} b_{42}^{(k,l)} - b_{43}^{(k,l)} b_{32}^{(k,l)}} \times (b_{41}^{(k,l)} b_{32}^{(k,l)} - b_{31}^{(k,l)} b_{42}^{(k,l)}, b_{44}^{(k,l)} b_{32}^{(k,l)} - b_{34}^{(k,l)} b_{42}^{(k,l)}, y_3 b_{42}^{(k,l)} - y_4 b_{32}^{(k,l)}),$$

$$(c_{31}^{(k,l)}, c_{32}^{(k,l)}, c_{33}^{(k,l)}) = -\frac{1}{b_{24}^{(k,l)} + b_{22}^{(k,l)} c_{12}^{(k,l)} + b_{23}^{(k,l)} c_{22}^{(k,l)}} \times \left(\frac{16\gamma_{24} kl\beta^2}{3\pi^2}, b_{21}^{(k,l)} + b_{22}^{(k,l)} c_{11}^{(k,l)} + b_{23}^{(k,l)} c_{21}^{(k,l)}, b_{22}^{(k,l)} c_{13}^{(k,l)} + b_{23}^{(k,l)} c_{23}^{(k,l)} \right),$$

$$d_1^{(k,l)} = -(b_{12}^{(k,.l)} c_{12}^{(k,l)} c_{31}^{(k,l)} + b_{13}^{(k,l)} c_{22}^{(k,l)} c_{31}^{(k,l)} + b_{14}^{(k,l)} c_{31}^{(k,l)} - s^{(k,l)} c_{32}^{(k,l)})/(s^{(k,l)} c_{31}^{(k,l)}),$$

$$d_2^{(k,l)} = (b_{11}^{(k,l)} + b_{12}^{(k,l)} c_{11}^{(k,l)} + b_{12}^{(k,l)} c_{12}^{(k,l)} c_{32}^{(k,l)} + b_{13}^{(k,l)} c_{21}^{(k,l)} + b_{13}^{(k,l)} c_{22}^{(k,l)} c_{32}^{(k,l)} + b_{14}^{(k,l)} c_{32}^{(k,l)} - s^{(k,l)} c_{33}^{(k,l)})/(s^{(k,l)} c_{31}^{(k,l)}),$$

$$d_3^{(k,l)} = (b_{12}^{(k,l)} c_{13}^{(k,l)} + b_{13}^{(k,l)} c_{23}^{(k,l)} + b_{14}^{(k,l)} c_{33}^{(k,l)} - y_1)/(s^{(k,l)} c_{31}^{(k,l)}),$$

$$q_{kl} = -d_3^{(k,l)} - \frac{2}{27}(d_1^{(k,l)})^2 + \frac{1}{3} d_1^{(k,l)} d_2^{(k,l)}, \quad p_{kl} = -d_2^{(k,l)} + (d_1^{(k,l)})^2/3,$$

$$s^{(k,l)} = \frac{32\gamma_{14} kl\beta^2}{3\pi^2},$$

$$y_1^{(k,l)} = M_x^{(0)} k/l + \beta^2 M_y^{(0)} l/k, \quad y_3^{(k,l)} = -S_x^{(0)}/l, \quad y_4^{(k,l)} = \beta S_y^{(0)}/k,$$

$$b_{11}^{(i,j)} = \gamma_{110}(im)^4 + 2\gamma_{112}(im)^2(jn)^2\beta^2 + \gamma_{114}(jn)^4\beta^4 - \gamma_{14}\beta^2(p_y m^2 + p_x n^2),$$

$$b_{12}^{(i,j)} = -[\gamma_{120}(im)^3 + \gamma_{122} im(jn)^2\beta^2],$$

$$b_{13}^{(i,j)} = -[\gamma_{131}(im)^2 jn\beta + \gamma_{133}(jn)^3\beta^3],$$

$$b_{14}^{(i,j)} = \gamma_{14}[\gamma_{140}(im)^4 + \gamma_{142}(im)^2(jn)^2\beta^2 + \gamma_{144}(jn)^4\beta^4],$$

$$b_{21}^{(i,j)} = -\gamma_{24}[\gamma_{240}(im)^4 + \gamma_{242}(im)^2(jn)^2\beta^2 + \gamma_{244}(jn)^4\beta^4],$$

$$b_{22}^{(i,j)} = \gamma_{24}[\gamma_{220}(im)^3 + \gamma_{222}(im)(jn)^2\beta^2],$$

$$b_{23}^{(i,j)} = \gamma_{24}[\gamma_{231}(im)^2(jn)\beta + \gamma_{233}(jn)^3\beta^3],$$

$$b_{24}^{(i,j)} = m^4 + 2\gamma_{212}(im)^2(jn)^2\beta^2 + \gamma_{214}(jn)^4\beta^4,$$

$$b_{31}^{(i,j)} = \gamma_{31}(im) - \gamma_{310}(im)^3 - \gamma_{312}(im)(jn)^2\beta^2,$$

$$b_{32}^{(i,j)} = \gamma_{31} + r_{320}(im)^2 + \gamma_{322}(jn)^2\beta^2,$$

$$b_{33}^{(i,j)} = \gamma_{331}(im)(jn)\beta,$$

$$b_{34}^{(i,j)} = -\gamma_{24}[\gamma_{220}(im)^3 + \gamma_{222}(im)(jn)^2\beta^2],$$

$$b_{41}^{(i,j)} = \gamma_{41}(jn)\beta - \gamma_{411}(im)^2(jn)\beta - \gamma_{413}(jn)^3\beta^3,$$

$$b_{42}^{(i,j)} = \gamma_{331}(im)(jn)\beta,$$

$$b_{43}^{(i,j)} = \gamma_{41} + r_{430}(im)^2 + \gamma_{432}(jn)^2\beta^2,$$

$$b_{44}^{(i,j)} = -\gamma_{14}[\gamma_{231}(im)^2(jn)\beta + \gamma_{233}(jn)^3\beta^3]. \tag{B.2}$$

In Eq. (36)

$$\begin{bmatrix} M_x^{(0)} & S_x^{(0)} \\ M_y^{(0)} & S_y^{(0)} \end{bmatrix} = \frac{16h}{\pi^2[D_{11}^* D_{22}^* A_{11}^* A_{22}^*]^{1/4}} \left(\begin{bmatrix} \gamma_{T3} & \gamma_{T3} - \gamma_{T6} \\ \gamma_{T4} & \gamma_{T4} - \gamma_{T7} \end{bmatrix} \bar{T} + \begin{bmatrix} \gamma_{P3} & \gamma_{P3} - \gamma_{P6} \\ \gamma_{P4} & \gamma_{P4} - \gamma_{P7} \end{bmatrix} \Delta V \right), \tag{B.3}$$

In Eqs. (43)–(47) (with $i,j = 1,3$)

$$\begin{aligned} B_{00}^{(0)} = & -\frac{1}{(\gamma_5^2 - \gamma_{24}^2)\beta^2} \left\{ [(\gamma_{24}^2\gamma_{T1} - \gamma_5\gamma_{T2}) + \gamma_5(\gamma_{T2} - \gamma_5\gamma_{T1})]\bar{T} \right. \\ & - \frac{4}{\pi^2} \sum_{k=1,3,\ldots} \sum_{l=1,3,\ldots} \frac{1}{kl} [(\gamma_5^2 - \gamma_{24}^2)n^2\beta^2 f_{kl} - \gamma_{24}(\gamma_{511} + \gamma_5\gamma_{220})m\psi_{kl} - \gamma_{24}(\gamma_{233} + \gamma_5\gamma_{522})n\beta\psi_{kl} \\ & \left. + \gamma_{24}(\gamma_{611}m^2 + \gamma_{244}n^2\beta^2)w_{kl} + \gamma_5\gamma_{24}(\gamma_{240}m^2 + \gamma_{622}n^2\beta^2)w_{kl}] \right\}, \end{aligned}$$

$$\begin{aligned} b_{00}^{(0)} = & -\frac{1}{(\gamma_5^2 - \gamma_{24}^2)} \left\{ [\gamma_5(\gamma_{24}^2\gamma_{T1} - \gamma_5\gamma_{T2}) + \gamma_{24}^2(\gamma_{T2} - \gamma_5\gamma_{T1})]\bar{T} \right. \\ & - \frac{4}{\pi^2} \sum_{k=1,3,\ldots} \sum_{l=1,3,\ldots} \frac{1}{kl} [(\gamma_5^2 - \gamma_{24}^2)m^2 f_{kl} - \gamma_{24}(\gamma_5\gamma_{511} + \gamma_{24}^2\gamma_{220})m\psi_{kl} - \gamma_{24}(\gamma_5\gamma_{233} + \gamma_{24}^2\gamma_{522})n\beta\psi_{kl} \\ & \left. + \gamma_5\gamma_{24}(\gamma_{611}m^2 + \gamma_{244}n^2\beta^2)w_{kl} + \gamma_{24}^3(\gamma_{240}m^2 + \gamma_{622}n^2\beta^2)w_{kl}] \right\}, \end{aligned}$$

$$g_{11}^{(i,j)} = \frac{k_{23}^{(i,j)}k_{31}^{(i,j)} - k_{33}^{(i,j)}k_{21}^{(i,j)}}{k_{22}^{(i,j)}k_{33}^{(i,j)} - k_{32}^{(i,j)}k_{23}^{(i,j)}},$$

$$g_{21}^{(i,j)} = \frac{k_{22}^{(i,j)}k_{31}^{(i,j)} - k_{32}^{(i,j)}k_{21}^{(i,j)}}{k_{23}^{(i,j)}k_{32}^{(i,j)} - k_{33}^{(i,j)}k_{22}^{(i,j)}},$$

$$g_{31}^{(i,j)} = a_1^{(i,j)} + b_1^{(i,j)}g_{11}^{(i,j)} + c_1^{(i,j)}g_{21}^{(i,j)}$$

$$g_{402}=\frac{\gamma_{24}m^2n^2\beta^2}{2\left(16\gamma_{214}n^4\beta^4+\dfrac{64\gamma_{14}\gamma_{24}\gamma_{223}^2n^6\beta^6}{\gamma_{41}+4\gamma_{432}n^2\beta^2}\right)},\quad g_{420}=\frac{\gamma_{24}m^2n^2\beta^2}{2\left(16m^4+\dfrac{64\gamma_{14}\gamma_{24}\gamma_{220}^2m^6}{\gamma_{31}+4\gamma_{320}m^2}\right)},$$

$$g_{12}=-\frac{8\gamma_{220}\gamma_{14}m^3}{\gamma_{31}+4\gamma_{320}m^2}\,g_{420},\quad g_{22}=-\frac{8\gamma_{233}\gamma_{14}n^3\beta^3}{\gamma_{41}+4\gamma_{432}n^2\beta^2}\,g_{402},$$

$$g_{441}=8g_{12}\gamma_{120}m^3+16g_{420}\gamma_{14}\gamma_{140}m^4+g_{31}^{(1,1)}\gamma_{14}\beta^2m^2n^2,$$

$$g_{442}=8g_{22}\gamma_{133}n^3\beta^3+16g_{420}\gamma_{14}\gamma_{144}n^4\beta^4+g_{31}^{(1,1)}\gamma_{14}\beta^2m^2n^2,$$

$$B_{00}^{(2)}=\frac{\gamma_{24}(m^2+\gamma_5n^2\beta^2)}{8(\gamma_5^2-\gamma_{24}^2)\beta^2},\quad b_{00}^{(2)}=\frac{\gamma_{24}(\gamma_5m^2+\gamma_{24}^2n^2\beta^2)}{8(\gamma_5^2-\gamma_{24}^2)}$$

$$g_{311}=\frac{\gamma_{14}\beta^2(m^2B_{00}^{(2)}+n^2b_{00}^{(2)})-2m^2n^2\gamma_{14}\beta^2(g_{402}+g_{420})}{k_{11}^{(1,1)}+k_{12}^{(1,1)}g_{11}^{(1,1)}+k_{13}^{(1,1)}g_{21}^{(1,1)}-\gamma_{14}\beta^2(m^2B_{00}^{(0)}+n^2b_{00}^{(0)}+s^{(1,1)})},$$

$$g_{331}=\frac{2\gamma_{14}m^2n^2\beta^2}{k_{11}^{(3,1)}+k_{12}^{(3,1)}g_{11}^{(3,1)}+k_{13}^{(3,1)}g_{21}^{(3,1)}-\gamma_{14}\beta^2(9m^2B_{00}^{(0)}+n^2b_{00}^{(0)}+s^{(3,1)})}\,g_{420},$$

$$g_{313}=\frac{2\gamma_{14}m^2n^2\beta^2}{k_{11}^{(1,3)}+k_{12}^{(1,3)}g_{11}^{(1,3)}+k_{13}^{(1,3)}g_{21}^{(1,3)}-\gamma_{14}\beta^2(m^2B_{00}^{(0)}+9n^2b_{00}^{(0)}+s^{(1,3)})}\,g_{402},$$

$$g_1=\frac{-b_2k_{13}^{(1,1)}(k_{12}^{(1,1)}k_{33}^{(1,1)}-k_{32}^{(1,1)}k_{13}^{(1,1)})+b_3k_{13}^{(1,1)}(k_{12}^{(1,1)}k_{23}^{(1,1)}-k_{22}^{(1,1)}k_{13}^{(1,1)})}{(k_{11}^{(1,1)}k_{23}^{(1,1)}-k_{21}^{(1,1)}k_{13}^{(1,1)})(k_{12}^{(1,1)}k_{33}^{(1,1)}-k_{32}^{(1,1)}k_{13}^{(1,1)})-(k_{11}^{(1,1)}k_{33}^{(1,1)}-k_{31}^{(1,1)}k_{13}^{(1,1)})(k_{12}^{(1,1)}k_{23}^{(1,1)}-k_{22}^{(1,1)}k_{13}^{(1,1)})},$$

$$g_2=\frac{-b_2k_{13}^{(1,1)}(k_{11}^{(1,1)}k_{33}^{(1,1)}-k_{31}^{(1,1)}k_{13}^{(1,1)})+b_3k_{13}^{(1,1)}(k_{11}^{(1,1)}k_{23}^{(1,1)}-k_{21}^{(1,1)}k_{13}^{(1,1)})}{(k_{12}^{(1,1)}k_{23}^{(1,1)}-k_{22}^{(1,1)}k_{13}^{(1,1)})(k_{11}^{(1,1)}k_{33}^{(1,1)}-k_{31}^{(1,1)}k_{13}^{(1,1)})-(k_{12}^{(1,1)}k_{33}^{(1,1)}-k_{32}^{(1,1)}k_{13}^{(1,1)})(k_{11}^{(1,1)}k_{23}^{(1,1)}-k_{21}^{(1,1)}k_{13}^{(1,1)})},$$

$$g_3=-\frac{k_{11}^{(1,1)}g_1+k_{12}^{(1,1)}g_2}{k_{13}^{(1,1)}},\quad g_4=a_1^{(1,1)}g_1+b_1^{(1,1)}g_2+c_1^{(1,1)}g_3,$$

$$g_{41}=k_{11}^{(1,1)}+k_{12}^{(1,1)}g_{11}^{(1,1)}+k_{13}^{(1,1)}g_{21}^{(1,1)}-\gamma_{14}\beta^2(m^2B_{00}^{(0)}+n^2b_{00}^{(0)}+s^{(1,1)}),$$

$$g_{42}=-\gamma_{14}\beta^2[m^2B_{00}^{(2)}+n^2b_{00}^{(2)}-2m^2n^2(g_{402}+g_{420})],$$

$$g_{43}=-(\gamma_{170}-\gamma_{171}m^2-\gamma_{171}n^2\beta^2-\gamma_{80}mg_{11}^{(1,1)}-\gamma_{80}n\beta g_{21}^{(1,1)}),$$

$$g_{44} = -\frac{2}{\pi^2 mn}\left[g_{441}(1-\cos m\pi)\left(\frac{2}{3}+\frac{1}{3}\cos 3m\pi-\cos m\pi\right)\right.$$
$$\left.+g_{442}(1-\cos n\pi)\left(\frac{2}{3}+\frac{1}{3}\cos 3n\pi-\cos n\pi\right)\right]-\gamma_{14}\beta^2(B_{00}^{(2)}m^2+b_{00}^{(2)}n^2)w_{mn},$$

$$B_{00}^{(2)}=\frac{\gamma_{24}(m^2+\gamma_5 n^2\beta^2)}{8(\gamma_5^2-\gamma_{24}^2)\beta^2},\quad b_{00}^{(2)}=\frac{\gamma_{24}(\gamma_5 m^2+\gamma_{24}^2 n^2\beta^2)}{8(\gamma_5^2-\gamma_{24}^2)}, \tag{B.4}$$

where

$$s^{(m,n)}=\frac{2}{\pi^2}\sum_{k=1,3,\ldots}\sum_{l=1,3,\ldots}\left[2(k^2n^2+l^2m^2)\left(\frac{1}{k}-\frac{1}{2k+4m}-\frac{1}{2k-4im}\right)\left(\frac{1}{l}-\frac{1}{2l+4n}-\frac{1}{2l-4n}\right)\right.$$
$$\left.-klmn\left(\frac{1}{2m+k}+\frac{1}{2m-k}\right)\left(\frac{1}{2n+l}+\frac{1}{2n-l}\right)(g_{13}^{(k,l)}w_{kl}+f_{kl}),\right]$$

$$b_2=\gamma_{90}m+\gamma_{10}g_{11}^{(1,1)},\quad b_3=\gamma_{90}n\beta+\gamma_{10}g_{21}^{(1,1)}. \tag{B.5}$$

In the above Eqs. (B.2)–(B.5)

$$k_{11}^{(i,j)}=\gamma_{110}(im)^4+2\gamma_{112}(im)^2(jn)^2\beta^2+\gamma_{114}(jn)^4\beta^4+\gamma_{14}[\gamma_{140}(im)^4+\gamma_{142}(im)^2(jn)^2\beta^2$$
$$+\gamma_{144}(jn)^4\beta^4]a_1^{(i,j)}-\alpha_1\gamma_{14}\beta^2(B_{00}^{(0)}m^2+b_{00}^{(0)}n^2),$$

$$k_{12}^{(i,j)}=-[\gamma_{120}(im)^3+\gamma_{122}im(jn)^2\beta^2]+\gamma_{14}[\gamma_{140}(im)^4+\gamma_{142}(im)^2(jn)^2\beta^2+\gamma_{144}(jn)^4\beta^4]b_1^{(i,j)},$$

$$k_{13}^{(i,j)}=-[\gamma_{131}(im)^2jn\beta+\gamma_{133}(jn)^3\beta^3]+\gamma_{14}[\gamma_{140}(im)^4+\gamma_{142}(im)^2(jn)^2\beta^2+\gamma_{144}(jn)^4\beta^4]c_1^{(i,j)},$$

$$k_{21}^{(i,j)}=\gamma_{31}im-\gamma_{310}(im)^3-\gamma_{312}im(jn)^2\beta^2-\gamma_{14}[\gamma_{220}(im)^3+\gamma_{222}(im)(jn)^2\beta^2]a_1^{(i,j)},$$

$$k_{22}^{(i,j)}=\gamma_{31}+r_{320}(im)^2+\gamma_{322}(jn)^2\beta^2-\gamma_{14}[\gamma_{220}(im)^3+\gamma_{222}(im)(jn)^2\beta^2]b_1^{(i,j)},$$

$$k_{23}^{(i,j)}=\gamma_{331}(im)(jn)\beta-\gamma_{14}[\gamma_{220}(im)^3+\gamma_{222}(im)(jn)^2\beta^2]c_1^{(i,j)},$$

$$k_{31}^{(i,j)}=\gamma_{41}jn\beta-\gamma_{411}(im)^2jn\beta-\gamma_{413}(jn)^3\beta^3-\gamma_{14}[\gamma_{231}(im)^2(jn)\beta+\gamma_{233}(jn)^3\beta^3]a_1^{(i,j)},$$

$$k_{32}^{(i,j)}=\gamma_{331}(im)(jn)\beta-\gamma_{14}[\gamma_{231}(im)^2(jn)\beta+\gamma_{233}(jn)^3\beta^3]b_1^{(i,j)},$$

$$k_{33}^{(i,j)}=\gamma_{41}+r_{430}(im)^2+\gamma_{432}(jn)^2\beta^2-\gamma_{14}[\gamma_{231}(im)^2(jn)\beta+\gamma_{233}(jn)^3\beta^3]c_1^{(i,j)}. \tag{B.6}$$

In Eq. (B.6), when w_{kl}, ψ_{xkl}, ψ_{ykl} and f_{kl} are considered, $\alpha_1 = 1$, otherwise $\alpha_1 = 0$, and

$$a_1^{(i,j)} = -\frac{\gamma_{24}}{m^4 + 2\gamma_{212}(im)^2(jn)^2\beta^2 + \gamma_{214}(jn)^4\beta^4}\left\{\gamma_{240}(im)^4 + \gamma_{242}(im)^2(jn)^2\beta^2 + \gamma_{244}(jn)^4\beta^4 + \frac{2\beta^2}{\pi^2}\sum_{k=1,3,\ldots}\sum_{l=1,3,\ldots}\left[2(k^2n^2 + l^2m^2)\left(\frac{1}{k} - \frac{1}{2k+4m} - \frac{1}{2k-4m}\right)\left(\frac{1}{l} - \frac{1}{2l+4n} - \frac{1}{2l-4n}\right) - mnkl\left(\frac{1}{2m+k} + \frac{1}{2m-k}\right)\left(\frac{1}{2n+l} - \frac{1}{2n-l}\right)\right]w_{kl}\right\},$$

$$b_1^{(i,j)} = -\frac{\gamma_{24}[\gamma_{220}(im)^3 + \gamma_{222}(im)(jn)^2\beta^2]}{m^4 + 2\gamma_{212}(im)^2(jn)^2\beta^2 + \gamma_{214}(jn)^4\beta^4},$$

$$c_1^{(i,j)} = -\frac{\gamma_{24}[\gamma_{231}(im)^2(jn)\beta + \gamma_{233}(jn)^3\beta^3]}{m^4 + 2\gamma_{212}(im)^2(jn)^2\beta^2 + \gamma_{214}(jn)^4\beta^4}. \quad \text{(B.7)}$$

References

[1] G.N. Praveen, J.N. Reddy, Nonlinear transient thermoelastic analysis of functionally graded ceramic–metal plates, *International Journal of Solids and Structures* 35 (1998) 4457–4476.

[2] Z.-Q. Cheng, R.C. Batra, Exact correspondence between eigenvalues of membranes and functionally graded simply supported polygonal plates, *Journal of Sound and Vibration* 229 (2000) 879–895.

[3] J. Yang, H.-S. Shen, Vibration characteristic and transient response of shear-deformable functionally graded plates in thermal environment, *Journal of Sound and Vibration* 255 (2002) 579–602.

[4] J. Yang, H.-S. Shen, Free vibration and parametric resonance of shear deformable functionally graded cylindrical panels, *Journal of Sound and Vibration* 261 (2003) 871–893.

[5] K.-S. Kim, N. Noda, A Green's function approach to the deflection of a FGM plate under transient thermal loading, *Archive of Applied Mechanics* 72 (2002) 127–137.

[6] Z.-Q. Cheng, J.N. Reddy, Frequency of functionally graded plates with three-dimensional asymptotic approach, *Journal of Engineering Mechanics* 129 (2003) 896–900.

[7] G.R. Liu, J. Tani, T. Ohyoshi, Lamb waves in a functionally gradient material plates and its transient response—Part 1: theory, Part 2: calculation results, *Transactions of the Japan Society of Mechanical Engineers* 57 (A) (1991) 603–611.

[8] G.R. Liu, X. Han, K.Y. Lam, Stress waves in functionally gradient materials and its use for material characterization, *Composites Part B* 30 (1999) 383–394.

[9] G.R. Liu, J. Tani, Characteristics of wave propagation in functionally graded piezoelectric material plates and its response analysis—Part 1: theory, Part 2: calculation results, *Transactions of the Japan Society of Mechanical Engineers* 57 (A) (1991) 2122–2133.

[10] G.R. Liu, J. Tani, Surface waves in functionally gradient piezoelectric material plates, *Journal of Vibration and Acoustics* 116 (1994) 440–448.

[11] G.R. Liu, K.Y. Dai, X. Han, T. Ohyoshi, Dispersion and characteristics of waves in functionally graded piezoelectric plates, *Journal of Sound and Vibration* 268 (2003) 131–147.

[12] X.Q. He, T.Y. Ng, S. Sivashanker, K.M. Liew, Active control of FGM plates with integrated piezoelectric sensors and actuators, *International Journal of Solids and Structures* 38 (2001) 1641–1655.

[13] K.M. Liew, X.Q. He, T.Y. Ng, S. Sivashanker, Active control of FGM plates subjected to a temperature gradient: modelling via finite element method based on FSDT, *International Journal for Numerical Methods in Engineering* 52 (2001) 1253–1271.
[14] K.M. Liew, X.Q. He, T.Y. Ng, S. Kitipornchai, Finite element piezothermoelasticity analysis and the active control of FGM plates with integrated piezoelectric sensors and actuators, *Computational Mechanics* 31 (2003) 350–358.
[15] K.M. Liew, S. Sivashanker, X.Q. He, T.Y. Ng, The modelling and design of smart structures using functionally graded materials and piezoelectric sensor/actuator patches, *Smart Materials and Structures* 12 (2003) 647–655.
[16] Y. Ootao, Y. Tanigawa, Three-dimensional transient piezothermoelasticity in functionally graded rectangular plate bonded to a piezoelectric plate, *International Journal of Solids and Structures* 37 (2000) 4377–4401.
[17] J.N. Reddy, Z.-Q. Cheng, Three-dimensional solutions of smart functionally graded plates, *Journal of Applied Mechanics* 68 (2001) 234–241.
[18] J. Yang, S. Kitipornchai, K.M. Liew, Large amplitude vibration of thermo-electric-mechanically stressed FGM laminated plates, *Computer Methods in Applied Mechanics and Engineering* 192 (2003) 3861–3885.
[19] J.N. Reddy, A refined nonlinear theory of plates with transverse shear deformation, *International Journal of Solids and Structures* 20 (1984) 881–896.
[20] H.-S. Shen, Kármán-type equations for a higher-order shear deformation plate theory and its use in the thermal postbuckling analysis, *Applied Mathematics and Mechanics* 18 (1997) 1137–1152.
[21] H.-S. Shen, Nonlinear bending response of functionally graded plates subjected to transverse loads and in thermal environments, *International Journal of Mechanical Sciences* 44 (2002) 561–584.
[22] H.-S. Shen, Postbuckling of shear deformable laminated plates with piezoelectric actuators under complex loading conditions, *International Journal of Solids and Structures* 38 (2001) 7703–7721.
[23] Y.S. Touloukian, *Thermophysical Properties of High Temperature Solid Materials*, MacMillan, New York, 1967.
[24] R. Javaheri, M.R. Eslami, Thermal buckling of functionally graded plates, *AIAA Journal* 40 (2002) 162–169.
[25] H.-S. Shen, Non-linear bending of shear deformable laminated plates under lateral pressure and thermal loading and resting on elastic foundations, *Journal of Strain Analysis for Engineering Design* 35 (2000) 93–108.
[26] H.-S. Shen, Thermal postbuckling of imperfect shear deformable laminated plates on two-parameter elastic foundations, *Mechanics of Composite Materials and Structures* 6 (1999) 207–228.
[27] X.-L. Huang, J.-J. Zheng, Nonlinear vibration and dynamic response of simply supported shear deformable laminated plates on elastic foundations, *Engineering Structures* 25 (2003) 1107–1119.
[28] H.-Q. Wang, *Nonlinear Vibration*, Higher Education Press, 1992 (in Chinese).
[29] C.E. Pearson, *Numerical Methods in Engineering and Science*, Van Nostrand Reinhold, New York, 1986.
[30] J.N. Reddy, C.D. Chin, Thermomechanical analysis of functionally graded cylinders and plates, *Journal of Thermal Stress* 21 (1998) 593–629.